ALMA MATER STUDIORUM - UNIVERSITÀ DI BOLOGNA

SCUOLA DI INGEGNERIA E ARCHITETTURA

DIPARTIMENTO DI INGEGNERIA INDUSTRIALE

CORSO DI LAUREA MAGISTRALE IN INGEGNERIA ENERGETICA

TESI DI LAUREA

in

Ingegneria dei Sistemi Superconduttivi

EXPANSION OF THE MAGNETIC FLUX DENSITY FIELD IN TOROIDAL HARMONICS

CANDIDATA

Laura Gambini

RELATORE

Prof. Ing. Marco Breschi

CORRELATORI

Dott. Ing. Luca Bottura
Dott. Ing. Enrico Felcini

Anno Accademico 2016/2017

Sessione III

Sommario

Il CERN (*Conseil Européen pour la Recherche Nucléaire*) è riconosciuto a livello mondiale come il principale laboratorio di ricerca nell'ambito della fisica delle particelle. Inevitabilmente, tutto ciò richiede l'impiego delle tecnologie più avanzate, sia dal punto di vista delle strumentazioni che delle metodologie analitico descrittive. Una delle molteplici potenzialità del lavoro che viene svolto al CERN riguarda la possibilità di sfruttare le suddette tecnologie anche in contesti che esulano dalla fisica delle particelle, con il risultato di influenzare l'avanzamento tecnologico di numerosi ambiti.

Ad esempio, una delle teorie più impiegate al CERN, per quanto riguarda la descrizione analitica del campo di induzione magnetica all'interno di magneti solenoidali (o approssimabili come tali sotto opportune ipotesi) per l'accelerazione di particelle, è la cosiddetta *espansione in multipoli*. Si tratta di una analisi di tipo bidimensionale o tridimensionale della distribuzione del campo generato dagli avvolgimenti di un magnete. Il magnete in questione può essere di tipo resistivo o superconduttivo; chiaramente, l'ambito in cui è impiegato non influenza in alcun modo l'applicabilità della teoria menzionata, purchè siano soddisfatti requisiti che riguardano principalmente la geometria del sistema.

La teoria dell'espansione in multipoli può essere impiegata anche nel caso di configurazioni magnetiche di tipo toroidale. Tuttavia, in questo caso è necessario sviluppare l'analisi in un sistema di coordinate molto più complesso e per nulla intuitivo.

In questo contesto si inserisce il lavoro della presente tesi, la quale si pone come obbiettivo lo sviluppo di una metodologia per la descrizione del campo di induzione magnetica generato da un magnete di tipo toroidale, impiegando la teoria dell'espansione in multipoli.

Lo studio inizia con una descrizione generale delle geometria toroidale e di alcune sue rilevanti applicazioni. Vengono inoltre descritti i possibili sistemi di coordinate impiegabili nel caso di magneti toroidali, col fine di individuare il set

di coordinate più adatto per l'espansione in multipoli.

A seguito di una panoramica sulla descrizione del campo di induzione magnetica generato da magneti solenoidali, lo studio si focalizza sulle trattazioni esistenti nel caso di magneti toroidali. Dopo un'accurata analisi, viene identificata la trattazione in grado di descrivere nella forma più generale possibile il campo di induzione magnetica all'interno del sistema, in modo da poter sfruttare questo studio per la maggior parte delle configurazioni toroidali esistenti e in fase di progetto. Il vantaggio principale di una descrizione analitica basata sull'espansione in multipoli riguarda la possibilità di identificare le componenti di campo di dipolo, quadrupolo, sestupolo, etc., tramite la valutazione dei coefficienti di multipolo (noti anche come momenti o coefficienti multipolari) che compaiono nell'espansione.

A causa delle complessità analitiche introdotte da questo tipo di trattazione e dalla geometria considerata, numerose verifiche sono necessarie per validare le espressioni delle componenti del campo di induzione magnetica.

Nella parte centrale del lavoro viene proposta una metodologia per il calcolo dei coefficienti multipolari, basata su procedure di *fitting*. L'unico requisito per l'applicazione di questa tecnica è la conoscenza dei valori di campo di induzione magnetica (o di potenziale scalare) in punti definiti di una superficie di forma toroidale. Viene inoltre introdotta una possibile strategia di tipo numerico per l'acquisizione dei valori del campo di induzione magnetica sui punti della griglia menzionata.

Infine, sono presentati e discussi i risultati ottenuti dall'applicazione della procedura di fitting proposta, nel caso di magneti toroidali formati da 8 e da 50 bobine.

Abstract

CERN (*Conseil Européen pour la Recherche Nucléaire*) is recognized worldwide as the main research laboratory in the field of particle physics. Inevitably, all this requires the use of the most advanced technologies, both from the point of view of the instruments and the analytical descriptive methods. One of the numerous potentials of the work carried out at CERN concerns the possibility of exploiting the aforementioned technologies even in contexts distant from the physics of particles, with the result of influencing the technological advancement of many areas.

For example, one of the most widely employed theories at CERN, regarding the analytical description of the magnetic flux density inside solenoidal magnets (or approximable as such under suitable assumptions) for the acceleration of particles, is the so-called *multipole expansion*. This is a two-dimensional or three-dimensional analysis of the distribution of the magnetic flux density generated by the windings of a magnet. The magnet in question can be either resistive or superconductive; clearly, the context in which it is employed does not influence the applicability of the aforementioned theory, provided that are satisfied requirements which mainly concern the geometry of the system.

The theory of multipole expansion can also be used in the case of toroidal magnetic configurations. However, in this case it is necessary to develop the analysis in a coordinate system much more complex and not at all intuitive.

In this context the work of the present thesis is inserted, which aims to develop a methodology for the description of the magnetic flux density generated by a toroidal magnet, using the theory of multipole expansion.

The study begins with a general description of the toroidal geometry and some of its relevant applications. The possible coordinate systems that can be used in the case of toroidal magnets are also described, in order to identify the most suitable coordinate set for the multipole expansion.

Following an overview of the magnetic flux density generated by solenoidal

magnets, the study focuses on the existing characterizations for what concerns toroidal magnets. After an accurate analysis, it is identified a characterization which allows to describe in the most general form the magnetic flux density inside the system, in order to exploit this study for most of the toroidal configurations, existing and in the design phase. The main advantage of an analytical description based on the expansion in multiples concerns the possibility of identifying the components of the dipole, quadrupole, sestupole, etc., by evaluating the multipole coefficients (also known as multipolar moments or coefficients) that appear expansion.

Because of the analytical complexities introduced by this type of description and the geometry considered, numerous verifications are necessary to validate the expressions of the magnetic flux density components.

In the central part of the work, a method for the calculation of multipolar coefficients is proposed; it is based on *fitting* procedures. The only requirement for the application of this technique is the knowledge of the magnetic flux density values (or of the scalar potential) in defined points of a toroidal shape surface. Furthermore, a possible numerical strategy is introduced for the acquisition of the magnetic flux density values on the points of the mentioned grid.

Finally, the results obtained from the application of the proposed fitting procedure are presented and discussed, in the case of toroidal magnets formed by 8 and 50 coils.

Contents

List of Figures

1. Toroidal configurations

This chapter provides an overview of the toroidal configurations, with particular attention on toroids and their applications. The coordinate sets that can be used to describe toroidal systems are also introduced.

1.1 Solenoids and toroids

A solenoid consists of a conductor wire tightly wound in the form of a spiral. In most applications, the wire is wrapped around a metallic core, called armature. As an electric current passes through the coils, a nearly uniform magnetic field is created, as *Figure 1.1* shows. The magnetic flux density (or magnetic induction), estimated as the sum of the magnetic flux density of individual turns of the conductor, is directed along the axis of the solenoid and can be approximated by:

$$B \approx \mu n I \tag{1.1}$$

where μ is the permeability of the core, $n = N/L$ is the number of turns (N) per unit length (L) and I is the current. Outside of the solenoid, the magnetic induction is far weaker. It can be noticed that the magnitude of the magnetic induction inside a solenoid, with a defined density of turns, is not dependent on the diameter of the magnet and is the same in every cross section; therefore solenoids can be used to create homogeneous magnetic fields [1].

The approximation *(1.1)* is valid only when the length of the magnet is much greater than its diameter. In the case of laboratory magnets the diameter of the hole is a few centimeters, while in experiments for high-energy physics it can be several meters.

When a solenoid is bent into the shape of a circle, it is called *toroid* (or *toroidal magnet*). This configuration produces a magnetic field whose field lines

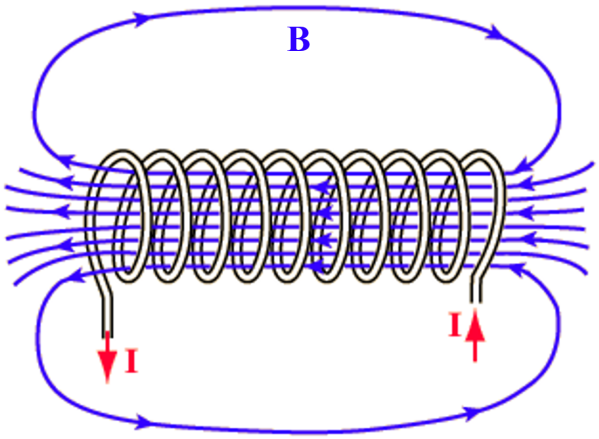

Figure 1.1 Simplified representation of the magnetic field generated by a solenoid.

are closed on themselves. An ideal toroidal magnet (*Figure 1.3* a) consists of a single spiral winding, with a uniform distribution of turns along the toroidal angle ϕ (also called *azimuthal coordinate*); consequently, the current density is uniform along ϕ. The magnetic field can be calculated by means of the Ampere's law:

$$\oint \mathbf{H} \cdot \mathbf{dl} = I \tag{1.2}$$

where I is the total current enclosed by the integration path; in the case of a toroidal magnet it is necessary to apply Ampere's law along three different integration paths, displayed in *Figure 1.2*:

- the path *inside* the torus (r_1), which does not enclose any current, hence the corresponding magnetic field H_1 is equal to zero;
- the path *through* the torus (r_2), which encloses N turns, with current I flowing in each of them, hence the corresponding magnetic field H_2 can be calculated as shown by equations *(1.3a)* and *(1.3b)*;

$$H_2\, 2\pi r_2 = NI \tag{1.3a}$$

$$H_2 = \frac{NI}{2\pi r_2} \tag{1.3b}$$

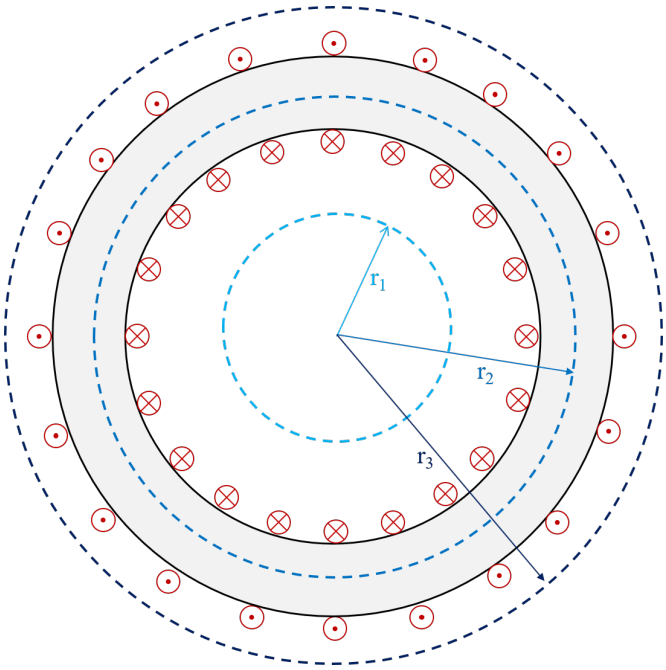

Figure 1.2 Representation of the integration paths on a toroid's section.

It can be seen that the resulting field is independent of the azimuthal coordinate ϕ and is inversely proportional to the radial distance from the z-axis;

- the path *outside* the torus (r_3), which encloses N turns carrying current in a same direction and N turns carrying current in the opposite direction, hence the total enclosed current is equal to zero; consequently also the corresponding magnetic field H_3 is equal to zero.

Applying the Ampere's law we have proved that the magnetic field of the ideal toroid is completely confined inside the magnet; moreover, because of the symmetry of the system, the radial and axial magnetic field components are absent. Therefore, the magnetic flux density of an ideal toroidal magnet can be described by equation *(1.4)*:

$$B_\phi = \frac{\mu_0 N I}{2\pi r} \tag{1.4}$$

A real toroidal magnet (*Figure 1.3* b) is built with a finite number of coils, for ease of fabrication and to allow access to the working volume. The magnetic field

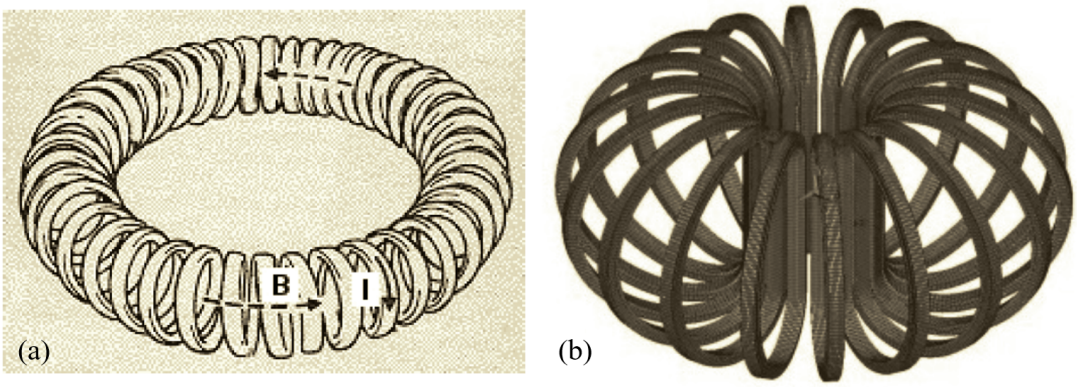

Figure 1.3 Ideal (a) and real (b) toroidal magnet.

of a torus composed of discrete coils turns out to have a dependence from the azimuthal coordinate, as will be explained in the following chapters.

1.2 Applications of toroidal magnets

Toroidal magnets are widely exploited in industry and in scientific research. In general, the most advantageous feature of this kind of configuration is the confinement of the magnetic field inside the magnet, this also allows to place toroids close to other machine, without concern about unwanted inductive interactions. Some significant applications are listed below.

1.2.1 Toroidal inductors

A toroidal inductor consists of an insulated wire wound around a toroidal shaped core of ferromagnetic material. Toroids are more efficient than solenoids in producing needed inductance, although their manufacture is more complicated; for the same inductance, a toroid requires fewer turns, hence it can be smaller in size than a solenoid with the same requirement [2].

1.2.2 SMES

The absence of external magnetic field makes the toroidal configuration suitable for the realization of *Superconducting Magnetic Energy Storage* (SMES), which store energy in the magnetic field created by the flow of current in a superconducting coil; SMES can be used to compensate voltage dips caused by

grid-connected renewable energy and to adjust power fluctuations created by faults in electric power systems. There are three main configurations of SMES: single-solenoid-type, multiple-solenoid-type and toroid-type, which is considered a suitable option for large-scale SMES [3].

1.2.3 Plasma confinement

Toroidal magnets are used in thermonuclear fusion studies. A tokamak is a torus-shaped vacuum chamber surrounded by magnetic coils, which create a strong toroidal magnetic field, that constrains charged particles to flow along that direction; a second set of coil is centered on the axis of the torus and generates a poloidal magnetic field which adds a vertical component that allows the control of the position of the plasma inside the torus; there is also a third magnetic field, generated by the plasma itself. This device is able to achieve the magnetic confinement of plasma, which is a key issue for nuclear fusion reactors, due to many instabilities of the system [4].

1.2.4 Particle detectors

Toroidal geometry is extensively exploited in the field of particle accelerators; for example, the magnetic system of ATLAS (*A Toroidal LHC ApparatuS*), one of the particle detectors in LHC (*Large Hadron Collider*) at CERN, comprises a central toroid, two end toroids and a central solenoid. The central toroid, called *barrel toroid*, is a large air-core magnet (outer diameter of 22 m) that produces a toroidal magnetic field of about 1.2 tesla [5].

1.2.5 Toroidal spectrometer

The TREK (*Time Reversal violation Experiment with Kaons*) detector, built at KEK (*High Energy Accelerator Research Organization*, Japan) is a significant example of toroidal spectrometer. The superconducting toroidal magnet present in this system consists of twelve iron sectors, each of which is magnetized by a superconducting coil; this setup provides a magnetic field of 1.8 T in the center of the magnet [6].

Another example of toroidal spectrometer is CLAS (*CEBAF Large Acceptance Spectrometer*) at CEBAF (*Continuous Electron Beams Accelerator Facility*, a linear accelerator of the Department of Energy's Thomas Jefferson

National Accelerator Facility, in Virginia). This detector is based on six superconducting coils disposed in a toroidal geometry around the beam line. At the maximum of the design current, the integral magnetic field reaches 2.5 Tm in the direction of the toroidal angle, with relevant deviations close to the coils [7].

The aim of both of these applications is to separate the trajectories of different particle by means of a toroidal field, depending on the momentum to charge ratio of the particles.

1.2.6 Magnetic horns

A magnetic horn is a device able to accept and select a strongly divergent beam of charged particles axisymmetric and to focus them to a nearly parallel beam, by means of an axisymmetric toroidal field. The original application of this system, invented at CERN, was related to neutrino physics [8].

1.2.7 Magnetic shield for astronauts

Toroidal magnetic field can be used also for space radiation shielding, to protect astronauts from charged particles due to *Solar Particle Events* (SPE), *Galatic Cosmic Rays* (GCR) and secondary cosmic rays. The most known and exploited solution for this problem is the *passive shielding*, it consist in positioning thin layers of specific material around the space cabin. This strategy results in large mass increasing, hence a valid alternative can be *active shielding*: in this case a device generates an electromagnetic field which deviates charged particles away from the space cabin. This kind of system consists of large superconducting magnets arranged around the space vessel; the most interesting and innovative solutions involve toroidal magnets. For instance, the SR2S design [9] is a novel configuration based on a set of toroidal magnet placed around the space cabin, with their axes directed radially.

1.3 Torus in Euclidean geometry

A torus is a surface of revolution obtained by revolving a circle about an axis coplanar with the circle, in a three-dimensional space of Euclidean geometry. In Cartesian coordinates, the implicit equation of a torus radially symmetric about

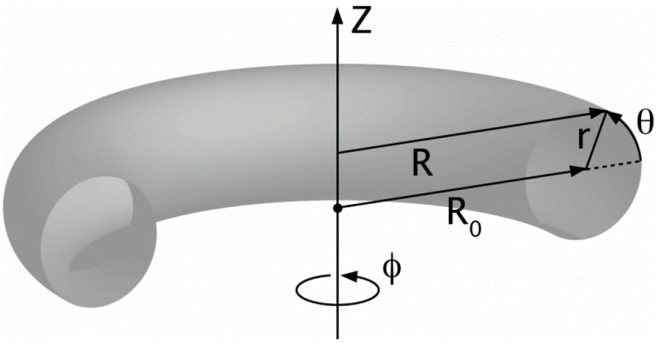

Figure 1.4 Representation of a toroidal geometry identified with elementary toroidal coordinates and cylindrical coordinates.

the z-axis is:

$$\left(R_0 - \sqrt{x^2 + y^2}\right)^2 + z^2 = r^2 \tag{1.5}$$

where R_0 (called *major radius*) is the distance between the center of the hole and the center of the tube, r (called *minor radius*) is the radius of the tube, as shown in *Figure 1.4*. Parametrically, a torus can be described by the equations:

$$x = (R_0 + r\cos\theta)\sin\phi \tag{1.6a}$$
$$y = (R_0 + r\cos\theta)\cos\phi \tag{1.6b}$$
$$z = r\sin\theta \tag{1.6c}$$

where θ is the poloidal angle and ϕ is the toroidal angle. The coordinate set consisting of r, θ and ϕ is called elementary toroidal system and is the most used coordinate system in cases of toroidal geometry [10]. A torus can also be expressed by means of a cylindrical coordinate system (R, ϕ, Z):

$$R^2 = x^2 + y^2 \tag{1.7a}$$
$$tan(\phi) = \frac{y}{x} \tag{1.7b}$$

However, as will be explained in chapter 3, the elementary toroidal system and the cylindrical system are not the best solutions when the aim is to find the description of the magnetic field inside a toroidal magnet. In this case it is appropriate to use a set of curvilinear coordinates called *toroidal coordinate system*, which can be obtained starting from the two-dimensional system of bipolar coordinates, as described in the following section.

1.4 Curvilinear coordinate system

Geometric considerations are not enough for the choice of the reference coordinate system, it is essential to take into account the physics of the problem. A set of coordinates $u = u(x, y, z)$, $v = v(x, y, z)$ and $w = w(x, y, z)$ [1], where u, v and w are orthogonal to each other, is called set of orthogonal curvilinear coordinates. The u_i should be single-valued, hence the reverse transformation $x_i = x_i(u, v, w)$ can be made. In some practical cases, for example when we are dealing with periodic functions on surfaces such as spheres, cylinders and tori, the single-valuedness doesn't hold; however, this problem can usually be circumvented [10].

A *metric coefficient* h_i (also called *scale factor*) is associated with each coordinate of an orthogonal coordinate system [11]. The square of an infinitesimal distance $\mathbf{s} = (x, y, z)$ can be written as:

$$(ds)^2 = (dx)^2 + (dy)^2 + (dz)^2 = h_u^2(du)^2 + h_v^2(dv)^2 + h_w^2(dw)^2 \tag{1.8}$$

where

$$h_u = \sqrt{\left(\frac{\partial x}{\partial u}\right) + \left(\frac{\partial y}{\partial u}\right) + \left(\frac{\partial z}{\partial u}\right)} \tag{1.9a}$$

$$h_v = \sqrt{\left(\frac{\partial x}{\partial v}\right) + \left(\frac{\partial y}{\partial v}\right) + \left(\frac{\partial z}{\partial v}\right)} \tag{1.9b}$$

$$h_w = \sqrt{\left(\frac{\partial x}{\partial w}\right) + \left(\frac{\partial y}{\partial w}\right) + \left(\frac{\partial z}{\partial w}\right)} \tag{1.9c}$$

[1] The set (x, y, z) represents the well known Cartesian coordinate system, whose unit vectors $\mathbf{i}$, $\mathbf{j}$ and $\mathbf{k}$ are constant in direction and magnitude.

Consequently, the unit vectors $\mathbf{e_i}$ associated with these coordinates can be expressed in the form:

$$\mathbf{e_u} = \frac{1}{h_u}\frac{\partial \mathbf{s}}{\partial u} \tag{1.10a}$$

$$\mathbf{e_v} = \frac{1}{h_v}\frac{\partial \mathbf{s}}{\partial v} \tag{1.10b}$$

$$\mathbf{e_w} = \frac{1}{h_w}\frac{\partial \mathbf{s}}{\partial w} \tag{1.10c}$$

In orthogonal curvilinear coordinates, the vector operators *gradient* ∇, *divergence* $\nabla\cdot$, *curl* $\nabla\times$ and *laplacian* ∇^2 are influenced by the scale factors [12]:

$$\nabla f = \frac{1}{h_u}\frac{\partial f}{\partial u}\mathbf{e_u} + \frac{1}{h_v}\frac{\partial f}{\partial v}\mathbf{e_v} + \frac{1}{h_w}\frac{\partial f}{\partial w}\mathbf{e_w} \tag{1.11}$$

$$\nabla \cdot \mathbf{F} = \frac{1}{h_u h_v h_w}\left[\frac{\partial}{\partial u}(F_u h_v h_w) + \frac{\partial}{\partial v}(F_v h_w h_u) + \frac{\partial}{\partial w}(F_w h_u h_v)\right] \tag{1.12}$$

$$\nabla \times \mathbf{F} = \frac{1}{h_u h_v h_w}\begin{vmatrix} h_u\mathbf{e_u} & h_v\mathbf{e_v} & h_w\mathbf{e_w} \\ \frac{\partial}{\partial u} & \frac{\partial}{\partial v} & \frac{\partial}{\partial w} \\ h_u F_u & h_v F_v & h_w F_w \end{vmatrix} \tag{1.13}$$

$$\nabla^2 f = \frac{1}{h_u h_v h_w}\left[\frac{\partial}{\partial u}\left(\frac{h_v h_w}{h_u}\frac{\partial f}{\partial u}\right) + \frac{\partial}{\partial v}\left(\frac{h_w h_u}{h_v}\frac{\partial f}{\partial v}\right) + \frac{\partial}{\partial w}\left(\frac{h_u h_v}{h_w}\frac{\partial f}{\partial w}\right)\right] \tag{1.14}$$

where f is a scalar field and $\mathbf{F} = (F_u, F_v, F_w)$ is a vector field.

1.4.1 Bipolar coordinates

Bipolar coordinates are a two-dimensional orthogonal coordinate system, based on two intersecting families of circles $\xi = constant$ and $\eta = constant$, as shown

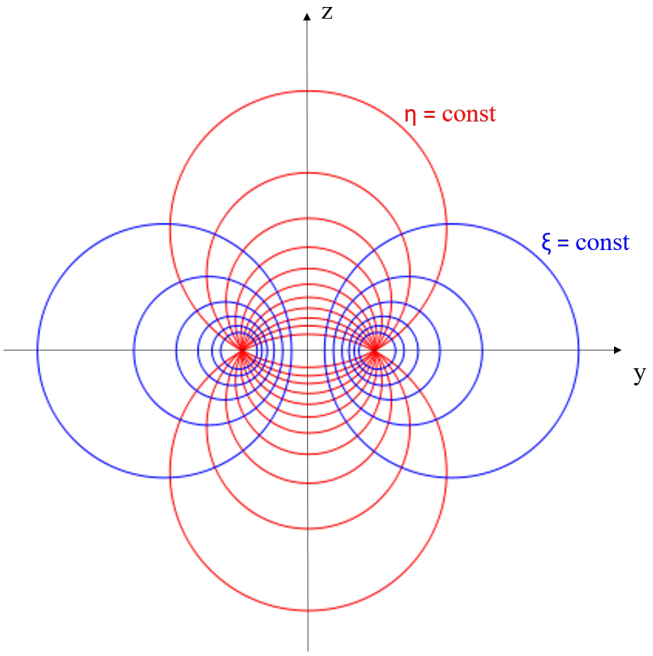

Figure 1.5 Bipolar coordinate system.

in *Figure 1.5*.

This coordinate system has two foci F_1 and F_2 located at $(-a, 0)$ and $(a, 0)$ respectively, in the y-axis of a Cartesian coordinate system. The coordinates ξ and η of a point P are defined as:

$$\xi = \ln\left(\frac{d_1}{d_2}\right) \qquad -\infty \leq \xi \leq \infty \tag{1.15a}$$

$$\eta = \alpha_1 - \alpha_2 \qquad 0 \leq \eta \leq 2\pi \tag{1.15b}$$

where d_1 and d_2 are the distances between the point P and each of the two foci F_1 and F_2; α_1 and α_2 are the angles between the y-axis and the lines F_1P and F_2P, respectively, as *Figure 1.6* shows.

The relations with Cartesian coordinates are:

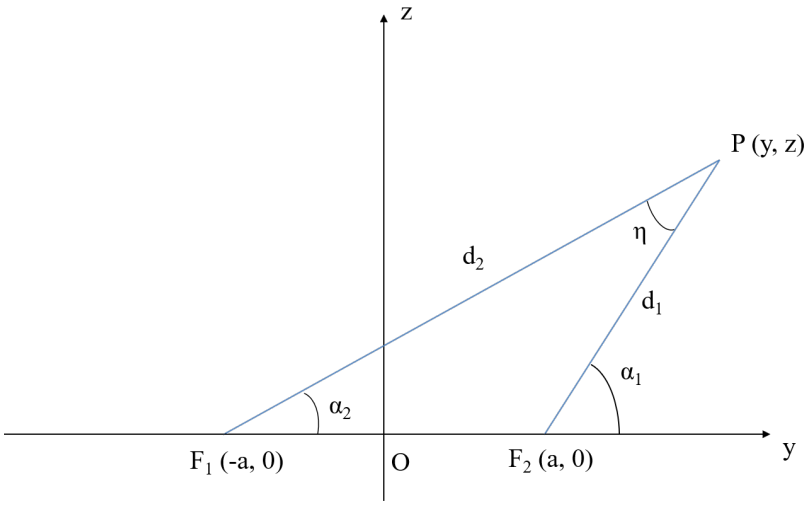

Figure 1.6 Representation of the parameters which define the bipolar coordinates.

$$y = \frac{a \sinh \xi}{\cosh \xi - \cos \eta} \tag{1.16a}$$

$$z = \frac{a \sin \eta}{\cosh \xi - \cos \eta} \tag{1.16b}$$

1.4.1.1 Coordinate curves

In curvilinear coordinate system, coordinate curves are produced allowing one coordinate to vary and holding fixed the other coordinate [10]. Coordinate curves of bipolar coordinate system are described below.

- Curves of constant η:

$$y^2 + (z - a \cot \eta)^2 = \frac{a^2}{\sin^2 \eta} \tag{1.17}$$

  are non-concentric circles that intersect at the two foci, with centers on the z-axis; circles of positive η have center above the y-axis, while circles of negative η have center below the y-axis. With the increasing of the magnitude $|a|$ the radius of the circles decreases and the center approaches

the origin $(0, 0)$, reached at $\frac{\pi}{2}$.

- Curves of constant ξ:

$$z^2 + (y - a\coth\xi)^2 = \frac{a^2}{\sinh^2\xi} \tag{1.18}$$

are non-concentric circles that surround one of the two foci, with centers on the y-axis; circles of positive ξ are located to the right of the z-axis ($y > 0$), while circles of negative ξ are located to the left of the z-axis ($y < 0$). As ξ increases, the radius of the circles decreases and their centers approach the foci; the $\xi = 0$ curve corresponds to the z-axis.

1.4.2 Toroidal coordinates

Toroidal coordinates (ξ, η, ϕ) are a three-dimensional coordinate system produced by rotating the two-dimensional bipolar coordinates around the z-axis. The foci F_1 and F_2 define a ring of radius $r = a$ placed in the xy plane; this focal ring is called *reference circle*. In this coordinate system, the position of any point is given by the intersection of a torus, a sphere and an azimuthal half plane, as shown in *Figure 1.7*.

1.4.2.1 Coordinate surfaces

In curvilinear coordinate systems, coordinate surfaces are obtained holding a coordinate fixed while the other two can vary [10]. Coordinate surfaces of toroidal coordinate system are described below.

- Surfaces of constant ξ:

$$z^2 + \left(\sqrt{x^2 + y^2} - a\coth\xi\right)^2 = \frac{a^2}{\sinh^2\xi} \tag{1.19}$$

are non intersecting tori generated by the rotation around the z-axis of circles C of radius $a/\sinh\xi$ centered at $r = a\coth\xi$. As ξ increases, the radius becomes smaller; when $\xi \to \infty$ the torus collapses to the reference

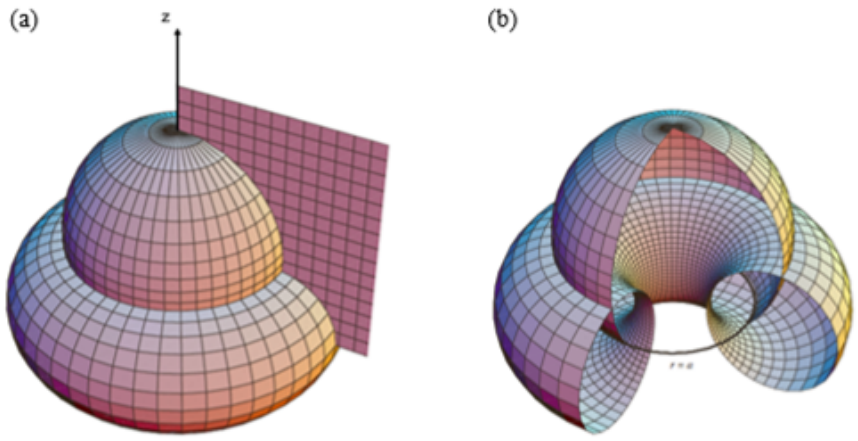

Figure 1.7 Toroidal coordinates: (a) intersection of a sphere, a torus and an half plane; (b) reference cirle.

circle ($r = a$, $z = 0$). When ξ decreases, the radius and the distance to the center of circle C become larger; in the limit of $\xi = 0$, the radius of the torus is infinite, the z-axis is identified as curve $\xi = 0$, because this is the part of the torus which is within a finite distance of the origin, when $\xi = 0$. The coordinate ξ can be seen as a radial coordinate, its range of variation is $0 \leq \xi < \infty$.

- Surfaces of constant η:

$$x^2 + y^2 + \left(z - a\cot\eta\right)^2 = \frac{a^2}{\sin^2\eta} \tag{1.20}$$

are spheres of radius $a/|\eta|$, with center at $z = a\cot\eta$, $r = 0$; these spheres intersect the $z = 0$ plane in the reference circle. The coordinate η can be interpreted as a sort of poloidal angle, its range of variation is $0 \leq \eta < 2\pi$.

- Surfaces of constant ϕ:

$$\tan\phi = \frac{y}{x} \tag{1.21}$$

are half planes denoting the rotation around the z-axis; the coordinate ϕ is exactly the toroidal angle defined in the elementary toroidal system, its range of variation is $0 \leq \phi < 2\pi$.

1.4.3 Correlations between Cartesian and toroidal coordinate system

The relations between toroidal and Cartesian coordinates are:

$$x = \frac{a \sinh \xi \cos \phi}{\cosh \xi - \cos \eta} = \frac{a \sinh \xi \cos \phi}{k} \tag{1.22a}$$

$$y = \frac{a \sinh \xi \sin \phi}{\cosh \xi - \cos \eta} = \frac{a \sinh \xi \sin \phi}{k} \tag{1.22b}$$

$$z = \frac{a \sin \eta}{\cosh \xi - \cos \eta} = \frac{a \sin \eta}{k} \tag{1.22c}$$

where $k = \cosh \xi - \cos \eta$.

The toroidal coordinates (ξ, η, ϕ) of a point P can be calculated from the Cartesian coordinates (x, y, z) as follow:

$$\xi = \ln\left(\frac{d_1}{d_2}\right) \tag{1.23a}$$

$$\cos \eta = -\frac{4a^2 - d_1^2 - d_2^2}{2 d_1 d_2} \tag{1.23b}$$

$$\tan \phi = \frac{y}{x} \tag{1.23c}$$

where

$$d_1^2 = (\rho + a)^2 + z^2 \tag{1.24a}$$

$$d_2^2 = (\rho - a)^2 + z^2 \tag{1.24b}$$

are the distance from P to F_1 and F_2, respectively, $|a|$ is the distance from each focus to the center of the coordinate system and $\rho = x^2 + y^2$ is the cylindrical radius of the point P.

In a toroidal coordinate system the scale factors, defined in the first part of this report, are:

$$h_\xi = h_\eta = \frac{a}{k} \tag{1.25a}$$

$$h_\phi = \frac{a \sinh \xi}{k} \tag{1.25b}$$

Consequently the unit vectors associated with this coordinate system are:

$$\mathbf{e}_\xi = \left(\frac{(1 - \cosh \xi \cos \eta) \cos \phi}{k}, \frac{(1 - \cosh \xi \cos \eta) \sin \phi}{k}, -\frac{\sinh \xi \sin \eta}{k} \right) \tag{1.26a}$$

$$\mathbf{e}_\eta = \left(-\frac{\sinh \xi \sin \eta \cos \phi}{k}, -\frac{\sinh \xi \sin \eta \sin \phi}{k}, \frac{\cosh \xi \cos \eta - 1}{k} \right) \tag{1.26b}$$

$$\mathbf{e}_\phi = \left(-\sin \phi, \cos \phi, 0 \right) \tag{1.26c}$$

It is possible to convert the components of a generic vector $\mathbf{B}$ from toroidal coordinates (B_ξ, B_η, B_ϕ) to Cartesian coordinates (B_x, B_y, B_z) and vice versa, by means of the following transformation matrix:

$$\begin{bmatrix} B_x \\ B_y \\ B_z \end{bmatrix} = \begin{bmatrix} \mathbf{e_x} \cdot \mathbf{e}_\xi & \mathbf{e_x} \cdot \mathbf{e}_\eta & \mathbf{e_x} \cdot \mathbf{e}_\phi \\ \mathbf{e_y} \cdot \mathbf{e}_\xi & \mathbf{e_y} \cdot \mathbf{e}_\eta & \mathbf{e_y} \cdot \mathbf{e}_\phi \\ \mathbf{e_z} \cdot \mathbf{e}_\xi & \mathbf{e_z} \cdot \mathbf{e}_\eta & \mathbf{e_z} \cdot \mathbf{e}_\phi \end{bmatrix} \begin{bmatrix} B_\xi \\ B_\eta \\ B_\phi \end{bmatrix} \tag{1.27}$$

where

$$\mathbf{e_x} = (1, 0, 0) \tag{1.28a}$$

$$\mathbf{e_y} = (0, 1, 0) \tag{1.28b}$$

$$\mathbf{e_z} = (0, 0, 1) \tag{1.28c}$$

are the unit vectors of the Cartesian coordinate system. Consequently, for the Cartesian components of the vector we obtain:

$$B_x = \frac{(1-\cosh\xi\cos\eta)\cos\phi}{k}B_\xi - \frac{\sinh\xi\sin\eta\cos\phi}{k}B_\eta - \sin\phi B_\phi \tag{1.29a}$$

$$B_y = \frac{(1-\cosh\xi\cos\eta)\sin\phi}{k}B_\xi - \frac{\sinh\xi\sin\eta\sin\phi}{k}B_\eta + \cos\phi B_\phi \tag{1.29b}$$

$$B_z = \frac{-\sinh\xi\sin\eta}{k}B_\xi + \frac{(\cosh\xi\cos\eta-1)}{k}B_\eta \tag{1.29c}$$

Analogously, with the inversion of the transformation matrix defined in *(1.27)*, it is possible to find the toroidal components of the vector $\mathbf{B}$:

$$B_\xi = \frac{(1-\cosh\xi\cos\eta)\cos\phi}{k}B_x + \frac{(1-\cosh\xi\cos\eta)\sin\phi}{k}B_y - \frac{\sinh\xi\sin\eta}{k}B_z \tag{1.30a}$$

$$B_\eta = -\frac{\sinh\xi\sin\eta\cos\phi}{k}B_x - \frac{\sinh\xi\sin\eta\sin\phi}{k}B_y + \frac{(\cosh\xi\cos\eta-1)}{k}B_z \tag{1.30b}$$

$$B_\xi = -\sin\phi B_x + \cos\phi B_y \tag{1.30c}$$

The important equations defined in section 1.4 can be written for a toroidal coordinate system as follow:

$$\nabla f = \frac{1}{a}(\cosh\xi-\cos\eta)\left[\frac{\partial f}{\partial\xi}\mathbf{e}_\xi + \frac{\partial f}{\partial\eta}\mathbf{e}_\eta + \frac{1}{\sinh\eta}\frac{\partial f}{\partial\phi}\mathbf{e}_\phi\right] \tag{1.31}$$

$$\nabla\cdot\mathbf{F} = \frac{(\cosh\xi-\cos\eta)^3}{a\sinh\xi)}\left[\frac{\partial}{\partial\xi}\left(\frac{\sinh\xi}{(\cosh\xi-\cos\eta)^2}F_\xi\right) + \sinh\xi\frac{\partial}{\partial\eta}\frac{F_\eta}{(\cosh\xi-\cos\eta)^2}\right] + \frac{(\cosh\xi-\cos\eta)}{a\sinh\xi}\frac{\partial}{\partial\phi}F_\phi \tag{1.32}$$

$$\nabla \times \mathbf{F} = \frac{(\cosh\xi - \cos\eta)^3}{a\sinh\xi} \begin{vmatrix} \mathbf{e}_\xi & \mathbf{e}_\eta & \sinh\xi\mathbf{e}_\phi \\ \frac{\partial}{\partial\xi} & \frac{\partial}{\partial\eta} & \frac{\partial}{\partial\phi} \\ \frac{F_\xi}{\cosh\xi-\cos\eta} & \frac{F_\eta}{\cosh\xi-\cos\eta} & \frac{F_\eta}{\cosh\xi-\cos\eta} \end{vmatrix} \tag{1.33}$$

$$\nabla^2 f = \frac{k^3}{a^2\sinh\xi}\left[\frac{\partial}{\partial\xi}\left(\frac{\sinh\xi}{k}\frac{\partial f}{\partial\xi}\right) + \sinh\xi\frac{\partial}{\partial\eta}\left(\frac{1}{k}\frac{\partial f}{\partial\eta}\right)\right] + \frac{k^2}{a^2\sinh^2\xi}\frac{\partial^2 f}{\partial\phi^2} = 0 \tag{1.34}$$

where f is a scalar field and $\mathbf{F} = (F_u, F_v, F_w)$ is a vector field.

2. 2D and 3D multipole expansion of the magnetic flux density in cylindrical and spherical coordinates

In this chapter, the formalism of the multipole expansion will be presented; it will be applied to describe the magnetic field inside a straight particle accelerator magnet, in two-dimensional and three-dimensional coordinate systems.

A function that depends on angles can be represented with a mathematical series called *multipole expansion* [13]. The series can be truncated at any order m, this means that only the first m terms of the expansion are used to approximate the function; as m increases, the approximation becomes more accurate. The expansion coefficients are called *multipole coefficients* or *multipolar moments*; the initial term of the series ($m = 0$) is the *monopole moment*, the second term ($m = 1$) is the *dipole moment*, the third term ($m = 2$) is the *quadrupole moment* and so on.

The multipole expansion is often used in studies of gravitational and electromagnetic fields; with this approximation is possible to describe the field quality in accelerator magnets, in a current free region. In this case, the multipolar moments are also called *field harmonics*. The procedure followed for the evaluation of the field harmonics is based on finding a general solution that satisfies the Laplace's equation, in a suitable coordinate system [14].

2.1 Two-dimensional multipole expansion

The measurement of the magnetic field is an important aspect of the development of particle accelerator magnets. In most cases we are interested in magnetic field in the aperture of the magnet, which is in vacuum and no current lines are present. Moreover, the majority of the accelerator magnets are long compared to their aperture, hence we can use a two-dimensional approach to study the distribution of the magnetic field. This approximation is not valid at the ends of the magnet [15].

In vacuum, without any current, the magnetic field $\mathbf{H}$ is irrotational (i.e. $\nabla \times \mathbf{H} = 0$). Also the magnetic induction (or *magnetic flux density*) $\mathbf{B} = \mu_0 \mathbf{H}$ (where $\mu_0 = 4\pi \times 10^{-7}$ Henry/m is the permeability of the free space) is irrotational and can be expressed as the gradient of a scalar function ψ, called *scalar potential*:

$$\nabla \times \mathbf{H} = 0 \Rightarrow \nabla \times \mathbf{B} = 0 \Rightarrow \mathbf{B} = -\nabla\psi \tag{2.1}$$

Furthermore, the magnetic induction $\mathbf{B}$ is solenoidal (i.e. $\nabla \cdot \mathbf{B} = 0$); consequently, we can write the Laplace's equation for the scalar potential:

$$\nabla^2 \psi = 0 \tag{2.2}$$

The scalar potential can therefore be expressed as a sum of orthogonal harmonics functions, in several curvilinear coordinate systems. For the purpose of simplicity, from here on, the magnetic flux density $\mathbf{B}$ will be called *magnetic field*, although it is known that magnetic field and magnetic flux density are different ($\mathbf{B} = \mu_0 \mathbf{H}$).

2.1.1 Expansion in cylindrical coordinates

In a cylindrical coordinate system (r, θ, z), equation *(2.2)* becomes:

$$\frac{1}{r}\frac{\partial}{\partial r}\left(r\frac{\partial \psi}{r}\right) + \frac{1}{r^2}\frac{\partial^2 \psi}{\partial \theta^2} + \frac{\partial^2 \psi}{\partial z^2} = 0 \tag{2.3}$$

We choose a cylindrical coordinate system with the origin centrally located in the magnet aperture and the z-axis along the length of the magnet. In this system, if we consider a two-dimensional magnetic field without axial component, the scalar

potential has no z-dependence. Therefore we obtain equation *(2.4)* which can be solved by separation of variables, with the boundary condition of periodicity of ψ in the coordinate θ and the finite value boundary condition at $r = 0$ [16].

$$r\frac{\partial}{\partial r}\left(r\frac{\partial \psi}{\partial r}\right) = -\frac{\partial^2 \psi}{\partial \theta^2} \tag{2.4}$$

$$\psi(r,\theta) = R(r)T(\theta) \tag{2.5}$$

We will provide here the resulting general solution *(2.6)*, which is a series expansion of the scalar potential; a detailed explanation can be found in [14].

$$\psi(r,\theta) = -\sum_{m=1}^{\infty} \frac{G_m}{m(R_{ref})^{m-1}} r^m \sin\Big(m(\theta - \alpha_m)\Big) \tag{2.6}$$

In equation *(2.6)*, G_m and α_m are constants and R_{ref} is an arbitrary radius, usually chosen to be $50 - 70\%$ of the magnet aperture.

According to the definition, the cylindrical components of the magnetic field can be obtained applying the gradient to the scalar potential. The radial and the angular components of the magnetic field can be written as:

$$B_r(r,\theta) = \sum_{m=1}^{\infty} G_m \left(\frac{r}{R_{ref}}\right)^{m-1} \sin\Big(m(\theta - \alpha_m)\Big) \tag{2.7a}$$

$$B_\theta(r,\theta) = \sum_{m=1}^{\infty} G_m \left(\frac{r}{R_{ref}}\right)^{m-1} \cos\Big(m(\theta - \alpha_m)\Big) \tag{2.7b}$$

The corresponding Cartesian components are most conveniently described in terms of a complex magnetic field $\mathbf{B}(z)$, defined as a function of the complex variable $z = x + iy$:

$$\mathbf{B}(z) = B_y(x,y) + iB_x(x,y) = \sum_{m=1}^{\infty} \Big[G_m e^{-in\alpha_m}\Big] \left(\frac{z}{R_{ref}}\right)^{m-1} \tag{2.8}$$

Equation *(2.8)* can be written in terms of *normal* A_m and *skew* B_m components of the magnetic field, defined as the real and the imaginary part of the expansion coefficients.

$$G_m e^{-in\alpha_m} = G_m \cos(m\alpha_m) - iG_m \sin(m\alpha_m) = B_m + iA_m \tag{2.9}$$

$$\mathbf{B}(z) = \sum_{m=1}^{\infty} \Big[B_m + iA_m\Big] \left(\frac{z}{R_{ref}}\right)^{m-1} \tag{2.10}$$

A magnet with the dominant term $2p - pole$ is called *normal* magnet if the $2p - pole$ skew term is zero. Vice versa, if the the $2p - pole$ normal term is zero the magnet is called *skew*. The values of the normal and skew components in *(2.10)*, or similarly the values of the amplitude G_m and the phase α_m in *(2.8)*, depend on the current distribution in the coils.

In the description of the field quality of a magnet, most of the time we are more interested in the shape of the field instead of its magnitude. For this purpose the terms of the expansion usually are expressed as a fraction of a *reference field* B_{ref}, which generally is chosen equal to the strength of the most dominant term of the expansion.

$$\mathbf{B}(z) = B_{ref} \sum_{m=1}^{\infty} \Big[\frac{G_m e^{-in\alpha_m}}{B_{ref}}\Big] \left(\frac{z}{R_{ref}}\right)^{m-1} \tag{2.11}$$

2.1.2 Expansion in spherical coordinates

It is possible to describe the magnetic field of a long accelerator magnet also using two-dimensional spherical coordinates (r, θ); the Laplace's equation *(2.2)* in this set of coordinates is written as:

$$r^2 \frac{\partial^2 \psi}{\partial r^2} + r \frac{\partial \psi}{r} + \frac{\partial^2 \psi}{\partial \theta^2} = 0 \tag{2.12}$$

The general solution is:

$$\psi(r, \theta) = \sum_{m=1}^{\infty} \Big(A_m r^m + B_m r^{-m}\Big)\Big(C_m \sin(m\theta) + D_n \cos(m\theta)\Big) \tag{2.13}$$

Applying the finite value boundary condition of the magnetic field at $r = 0$, that

implies $B_m = 0$, and arranging the coefficients, the general expression of the scalar potential *(2.13)* becomes:

$$\psi(r,\theta) = \sum_{m=1}^{\infty} r^m \Big(A_m \sin(m\theta) + B_m \cos(m\theta) \Big) \tag{2.14}$$

The radial and angular magnetic field components can be deduced as follow:

$$B_r(r,\theta) = -\mu_0 \frac{\partial \psi}{\partial r} = -\mu_0 \sum_{m=1}^{\infty} m r^{m-1} \Big(A_m \sin(m\theta) + B_m \cos(m\theta) \Big) \tag{2.15a}$$

$$B_\theta(r,\theta) = -\frac{\mu_0}{r} \frac{\partial \psi}{\partial \theta} = -\frac{\mu_0}{r} \sum_{m=1}^{\infty} m r^{m} \Big(A_m \cos(m\theta) - B_m \sin(m\theta) \Big) \tag{2.15b}$$

2.1.3 Evaluation of multipole coefficients

In the current section will be explained one of the most exploited method for the evaluation of the multipole coefficients, considering the solution of Laplace's equation in two-dimensional spherical coordinates. To apply this procedure it is necessary to calculate numerically or measure (for example by means of rotating induction coil) the radial component of the magnetic field at reference radius $r = r_0$, as a function of the angle θ [14]. The radial field component can now be expressed by means of Fourier series, as shown below:

$$B_r(r_0,\theta) = \sum_{m=1}^{\infty} \Big(C_m(r_0) \sin(m\theta) + D_m(r_0) \cos(m\theta) \Big) \tag{2.16}$$

where the Fourier coefficients $C_m(r_0)$ and $D_m(r_0)$ are evaluated as follow:

$$C_m(r_0) = \frac{1}{\pi} \int_0^{2\pi} B_r(r_0,\theta) cos(m\theta) d\theta \tag{2.17a}$$

$$D_m(r_0) = \frac{1}{\pi} \int_0^{2\pi} B_r(r_0,\theta) sin(m\theta) d\theta \tag{2.17b}$$

In computational practice, the Fourier coefficients are numerically calculated

applying the *Fourier Discrete Transform* (DFT), following the procedure described below [17]. The radial magnetic field component B_r is known at L discrete points in the range [0, 2π):

$$\theta_l = \frac{2\pi l}{L} \tag{2.18}$$

where $l = 0, 1, 2...(L-1)$; the minimum required value of L to obtain an accurate solution up to order $m = 15$ is $L = 60$ [14]. Applying the DFT to these points we can approximate the values of the Fourier coefficients:

$$C_m(r_0) \approx \frac{2}{L} \sum_{l=0}^{L-1} B_r(r_0, \theta_l) \cos(m\theta_l) \tag{2.19a}$$

$$D_m(r_0) \approx \frac{2}{L} \sum_{l=0}^{L-1} B_r(r_0, \theta_l) \sin(m\theta_l) \tag{2.19b}$$

The general expression of the radial magnetic field *(2.15a)*, written for the reference radius $r = r_0$, is:

$$B_r(r_0, \theta) = -\mu_0 \sum_{m=1}^{\infty} m r_0^{m-1} \Big(A_m \sin(m\theta) + B_m \cos(m\theta) \Big) \tag{2.20}$$

A comparison between the Fourier coefficients $C_m(r_0), D_m(r_0)$ of equation *(2.16)* and the coefficients A_m, B_m of equation *(2.20)* yields:

$$A_m = -\frac{C_m(r_0)}{\mu_0 m r_0^{m-1}} \tag{2.21a}$$

$$B_m = -\frac{D_m(r_0)}{\mu_0 m r_0^{m-1}} \tag{2.21b}$$

Therefore, the coefficients A_m, B_m introduced in the expression of the scalar potential *(2.14)* and in the expressions of the magnetic field components *(2.15a)* and *(2.15b)*, can be replaced with the expression obtained in equations *(2.21a)* and *(2.21b)*.

$$\psi(r,\theta) = -\frac{r_0}{\mu_0}\sum_{m=1}^{\infty}\frac{1}{m}\left(\frac{r}{r_0}\right)^m\Big(C_m(r_0)\sin(m\theta) + D_m(r_0)\cos(m\theta)\Big) \tag{2.22a}$$

$$B_r(r,\theta) = \sum_{m=1}^{\infty}\left(\frac{r}{r_0}\right)^{m-1}\Big(C_m\sin(m\theta) + D_m\cos(m\theta)\Big) \tag{2.22b}$$

$$B_\theta(r,\theta) = \sum_{m=1}^{\infty}\left(\frac{r}{r_0}\right)^{m-1}\Big(C_m\cos(m\theta) - D_m\sin(m\theta)\Big) \tag{2.22c}$$

We have expressed the scalar potential and the magnetic field components as a function of the multipoles evaluated with a Fourier series expansion at a reference radius r_0.

2.1.4 Vector Laplace's equation

For completeness, it is important to underline that the Laplace's equation *(2.2)* can be written also for a vector potential $\mathbf{A}$. From Maxwell's equations, it is known that the divergence of $\mathbf{B}$ is zero, hence we can express it as the curl of a vector $\mathbf{A}$, called *vector potential*:

$$\mathbf{B} = \nabla \times \mathbf{A} \tag{2.23}$$

The vector Laplace's equation *(2.25)* can be obtained, for a current-free region ($\nabla \times \mathbf{B} = 0$), applying the curl to equation *(2.23)*, with the choice of Coulomb gauge ($\nabla \cdot \mathbf{A} = 0$):

$$\nabla \times \mathbf{B} = \nabla \times (\nabla \times \mathbf{A}) = \nabla(\nabla \cdot \mathbf{A}) - \nabla^2\mathbf{A} = 0 \tag{2.24}$$

$$\nabla^2\mathbf{A} = 0 \tag{2.25}$$

This equation can be solved in two-dimensional spherical coordinates to find the magnetic field in the aperture of a long accelerator magnet. Far from the ends of the magnet, we can approximate the vector potential with its components A_z. The Laplace's equation can be solved by separation of variables, as follow:

$$A_z = \rho(r)\Theta(\theta) \tag{2.26}$$

The resulting general solution is:

$$A_z(r,\theta) = \sum_{m=1}^{\infty} (A_m r^m + B_m r^{-m})(C_m \sin(m\theta) + D_m \cos(m\theta)) \tag{2.27}$$

As for the solution of the scalar Laplace's equation, also in this case the term B_m is set equal to zero to satisfy the finite value boundary condition at $r = 0$; arranging the coefficients, equation *(2.27)* becomes:

$$A_z(r,\theta) = \sum_{m=1}^{\infty} r^m (A_m \sin(m\theta) + B_m \cos(m\theta)) \tag{2.28}$$

which is equal to the solution obtained for the scalar potential *(2.14)*. However, since in the present description the magnetic field is expressed as the curl of a vector function and not as the gradient of a scalar function, the expressions of the magnetic field components are different from the description of *Section* 2.1.2.

$$B_r(r,\theta) = \frac{1}{r}\frac{\partial A_z}{\partial \theta} = \sum_{m=1}^{\infty} m r^{m-1}\Big(A_m \cos(m\theta) - B_m \sin(m\theta)\Big) \tag{2.29a}$$

$$B_\theta(r,\theta) = -\frac{\partial A_z}{\partial \theta} = -\sum_{m=1}^{\infty} m r^{m-1}\Big(A_m \sin(m\theta) + B_m \cos(m\theta)\Big) \tag{2.29b}$$

2.2 Three-dimensional multipole expansion

At the ends of the magnets, the two-dimensional approximation is no longer valid, therefore it is necessary to solve the Laplace's equation in a three-dimensional coordinate system. For instance, in cylindrical coordinates the general solution of the scalar Laplace's equation is:

$$\psi(r,\theta,z) = \sum_{m=1}^{\infty}\sum_{p=1}^{\infty} I_n(pr)\Big[\Big(E_{p,n}\cos(pz) + F_{p,n}\sin(pz)\Big)\cos(n\theta) + \Big(G_{p,n}\cos(pz) + H_{p,n}\sin(pz)\Big)\sin(n\theta)\Big] \quad (2.30)$$

where

$$I_n(pr) = \sum_{k=0}^{\infty} \frac{1}{k!\Gamma(k+n+1)}\Big(\frac{pr}{2}\Big)^{n+2k} \quad (2.31)$$

is the modified Bessel function of the first kind [18]. This three-dimensional study allows to find numerically a description of the magnetic field, but requires the introduction of recursion relations to evaluate the expansion coefficients and the introduction of the so called *pseudo multipoles*. A detailed explanation can be found in [14].

3. Multipole expansion of the magnetic flux density in toroidal coordinates: the state of the art

As mentioned above, the magnetic field generated by a real toroidal magnet is different from the magnetic field of an ideal toroidal magnet, described by equation *(1.4)*. To obtain a wider description of the magnetic field, which can also be extended to real toroidal magnets, it is advisable to follow a procedure based on the multipole expansion method introduced in the previous chapter, with the appropriate modification required by the toroidal configuration. The aim of the current chapter is to provide an overview of this procedure and of some possibilities to employ it.

3.1 Laplace's equation in toroidal coordinates

The internal region[1] of a toroidal magnet is current-free as the central part of the straight magnet examined in chapter 2, hence, even in this case of study, it is possible to introduce a scalar potential ψ, related to the magnetic field, that satisfies the Laplace's equation *(3.2)*. For convenience, in this case the sign of the gradient of the scalar potential is defined concord with the magnetic field, unlike what has been proposed in the previous chapter (equation *(2.1)*).

$$\mathbf{B} = \nabla\psi \tag{3.1}$$

$$\nabla^2\psi = 0 \tag{3.2}$$

The choice of the coordinate system in which solve the Laplace's equation must be

[1] With the term *internal* we mean the area inside the coils of the magnet.

consistent with the geometry of the region of interest. Therefore, for our study it is appropriate to adopt the toroidal coordinate system described in section 1.4.2. The Laplace's equation in toroidal coordinates (ξ, η, ϕ), obtained from the definitions provided in section 1.4.3, is expressed by:

$$\nabla^2\psi = \frac{k^3}{a^2 \sinh\xi}\left[\frac{\partial}{\partial\xi}\left(\frac{\sinh\xi}{k}\frac{\partial\psi}{\partial\xi}\right) + \sinh\xi\frac{\partial}{\partial\eta}\left(\frac{1}{k}\frac{\partial\psi}{\partial\eta}\right)\right] + \frac{k^2}{a^2\sinh^2\xi}\frac{\partial^2\psi}{\partial\phi^2} = 0 \quad (3.3)$$

where $k = cosh(\xi) - cos(\eta)$.

3.1.1 Brief overview of the resolution techniques of the Laplace's equation

The separation of variables proposed in the chapter 2 is known as *simple separation of variables*; it can be applied in eleven coordinate system: Cartesian, circular cylindrical, elliptic cylindrical, parabolic-cylindrical, spherical, prolate spheroidal, oblate spheroidal, parabolic, conical, ellipsoidal and paraboloidal coordinates [11].

Toroidal coordinates do not allow the simple separation; however, for the set of coordinate described in section 1.4.2 it is possible to solve the Laplace's equation introducing a multiplicative term R, called *modulation factor*, which improves the possibility of solving a differential equation by separation; this resolution technique is known as *R-separation*[2].

A partial differential equation with variables u_1, u_2, u_3 is said to be *simple separable* if the assumption:

$$\Phi = X_1(u_1)X_2(u_2)X_3(u_3) \quad (3.4)$$

allows the separation of the mentioned partial differential equation in three ordinary differential equations. If, instead, the equation that permits the separation is:

$$\Phi = \frac{X_1(u_1)X_2(u_2)X_3(u_3)}{R(u_1, u_2, u_3)} \quad (3.5)$$

[2]This method can also be applied to bispherical coordinate system.

with $R \neq const$, the equation is called *R-separable*. The procedure to find R and the separated equations can be found in [11] and [19].

3.2 Toroidal harmonics

When the Laplace's equation is solved in the toroidal coordinate system, the harmonics fields are called *toroidal harmonics*. In this case, the modulation factor necessary for the R-separation is:

$$R = \frac{1}{\sqrt{(\cosh(\xi) - \cos(\eta))}} = k^{-\frac{1}{2}} \tag{3.6}$$

Employing the R-separation technique, equation *(3.2)* can be separated by replacing:

$$\psi = k^{\frac{1}{2}} f(\xi)\, g(\eta)\, h(\phi) \tag{3.7}$$

The separated equations are:

$$\frac{d^2 f}{d\xi^2} + \coth(\xi)\frac{df}{d\xi} + \left(\frac{1}{4} - m^2 - \frac{n^2}{\sinh^2(\xi)}\right) f = 0 \tag{3.8a}$$

$$\frac{d^2 g}{d\eta^2} + m^2 g = 0 \tag{3.8b}$$

$$\frac{d^2 h}{d\phi^2} + n^2 h = 0 \tag{3.8c}$$

whose solutions can be written in the most general form as:

$$f = \sum_{m=0}^{\infty}\sum_{n=0}^{\infty}\Big[A_{m,n}P^{n}_{m-\frac{1}{2}}(\cosh\xi) + B_{m,n}Q^{n}_{m-\frac{1}{2}}(\cosh\xi)\Big] \tag{3.9a}$$

$$g = \sum_{m=0}^{\infty}\Big[C_m\cos(m\eta) + D_m\sin(m\eta)\Big] \tag{3.9b}$$

$$h = \sum_{n=0}^{\infty}\Big[E_n\cos(n\phi) + F_n\sin(n\phi)\Big] \tag{3.9c}$$

where $P^{n}_{m-\frac{1}{2}}(\cosh\xi)$ and $Q^{n}_{m-\frac{1}{2}}(\cosh\xi)$ are the associated Legendre functions (called also Legendre polynomials) with half-integer indexes, whose definitions and properties will be investigated in Appendix A; m and n are separation indexes (non-negative integers); $A_{m,n}$, $B_{m,n}$, C_m, D_m, E_n and F_n are constants to be determined by imposing boundary conditions. The periodicity of the angular coordinates η and ϕ is assumed. The separated solutions *(3.9)* can be combined in order to write *(3.7)* as follow.

$$\begin{aligned}\psi = k^{\frac{1}{2}}\sum_{m=0}^{\infty}\sum_{n=0}^{\infty}&\Big[A_{m,n}P^{n}_{m-\frac{1}{2}}(\cosh\xi) + B_{m,n}Q^{n}_{m-\frac{1}{2}}(\cosh\xi)\Big]\\ &\times\Big[C_m\cos(m\eta) + D_m\sin(m\eta)\Big]\Big[E_n\cos(n\phi) + F_n\sin(n\phi)\Big]\end{aligned} \tag{3.10}$$

Equation *(3.10)* represents the general solution of the Laplace's equation in toroidal coordinates. The employment of toroidal harmonics is particularly convenient: the moments present in the scalar potential expression can be directly interpreted as field components of the dipole, quadrupole, sextupole, etc.; furthermore, studies were conducted on the link between current and multipolar moments [20].

The main disadvantage on the use of toroidal harmonics is the presence of associated Legendre functions with half-integer indexes, whose trend is difficult to evaluate. This is mostly because there is no universally recognized technique to calculate them, but different algorithms have been developed, which in some cases can lead to different results. For this reason, some authors have preferred to avoid using toroidal harmonics, trying to adapt different analytical descriptions (which can involve for instance the well-known Bessel functions) to toroidal geometry

systems [21] or modifying the expression of the scalar potential [22]. All these alternative strategies inevitably lead to approximations.

One of the most relevant study about multipole expansion in toroidal harmonics, was developed by *Lucas Brouwer* [23], who suggested the use of an algorithm called *DTOR* for the numerical evaluation of the Legendre functions [24]. In the mentioned work, equation *(3.10)* is written in a slightly different form, applying the sine and cosine addition formulas and arranging the coefficients:

$$\psi = k^{\frac{1}{2}} \sum_{m=0}^{\infty} \sum_{n=0}^{\infty} \Big[A_{m,n} P^n_{m-\frac{1}{2}}(\cosh \xi) + B_{m,n} Q^n_{m-\frac{1}{2}}(\cosh \xi) \Big] \times \Big[C_{m,n} \cos(m\eta - n\phi) + D_{m,n} \sin(m\eta + n\phi) \Big] \quad (3.11)$$

When we consider a torus surface of constant $\xi = \xi_0$, it is possible to write equation *(3.10)* separately for the internal and the external region of the torus [23].

$$\psi^{int}(\xi_0 < \xi < \infty) = k^{\frac{1}{2}} \sum_{m=0}^{\infty} \sum_{n=0}^{\infty} Q^n_{m-\frac{1}{2}}(\cosh \xi) \Big[C^{int}_{m,n} \cos(m\eta - n\phi) + D^{int}_{m,n} \sin(m\eta + n\phi) \Big] \quad (3.12)$$

$$\psi^{ext}(0 < \xi < \xi_0) = k^{\frac{1}{2}} \sum_{m=0}^{\infty} \sum_{n=0}^{\infty} P^n_{m-\frac{1}{2}}(\cosh \xi) \Big[C^{ext}_{m,n} \cos(m\eta - n\phi) + D^{ext}_{m,n} \sin(m\eta + n\phi) \Big] \quad (3.13)$$

This distinction is due to the requirement of finiteness of the Legendre polynomials at each point of the considered domain; it is indeed known that $P^n_{m-\frac{1}{2}}(\cosh \xi)$ presents a singularity when $\xi = \infty$, while $Q^n_{m-\frac{1}{2}}(\cosh \xi)$ is singular if $\xi = 0$. Assuming that the solution is symmetric about the $\eta = 0$ axis, the term $\sin(m\eta + n\phi)$ of equations *(3.12)* and *(3.13)* can be neglected; hence,

arranging the coefficients and considering the Einstein notation, it is possible to write:

$$\psi^{int}(\xi_0 < \xi < \infty) = k^{\frac{1}{2}} Q^n_{m-\frac{1}{2}}(\cosh\xi) A^{int}_{m,n} \cos(m\eta - n\phi) \tag{3.14}$$

$$\psi^{ext}(0 < \xi < \xi_0) = k^{\frac{1}{2}} P^n_{m-\frac{1}{2}}(\cosh\xi) A^{ext}_{m,n} \cos(m\eta - n\phi) \tag{3.15}$$

Applying the gradient (see section 1.4.3) to the scalar potential expression, we can obtain the magnetic field components. For instance, the internal magnetic field $\mathbf{B} = -\nabla\psi^{int}$ is described by:

$$B^{int}_{\xi} = -\frac{A^{int}_{m,n}}{a} k^{\frac{3}{2}} \left[Q^n_{m-\frac{1}{2}}(\cosh\xi) \left(\frac{m-\frac{1}{2}}{\tanh\xi} + \frac{\sinh\xi}{2k} \right) - Q^n_{m-\frac{3}{2}}(\cosh\xi) \frac{n+m-\frac{1}{2}}{\sinh\xi} \right] \cos(m\eta - n\phi) \tag{3.16}$$

$$B^{int}_{\eta} = -\frac{A^{int}_{m,n}}{a} k^{\frac{3}{2}} Q^n_{m-\frac{1}{2}}(\cosh\xi) \left(-m\sin(m\eta - n\phi) - \frac{\sin\eta\cos(m\eta - n\phi)}{2k} \right) \tag{3.17}$$

$$B^{int}_{\phi} = -\frac{n\, A^{int}_{m,n}}{a \sinh\xi} k^{\frac{3}{2}} Q^n_{m-\frac{1}{2}}(\cosh\xi)\, \sin(m\eta - n\phi) \tag{3.18}$$

where $|a|$ is the distance from each focus to the center of the toroidal coordinate system.

From these expressions we realize that the description of the magnetic field is incomplete, indeed it does not take into account the ideal component of the magnetic field $B_\phi = \frac{\mu_0 NI}{2\pi r}$ introduced in section 1.1. A complete description of the magnetic field, proposed by *B. Ph. van Milligen* in [25], will be investigated in the following section.

As mentioned in chapter 1.4.3, we can write the Laplace's equation also for the vector potential $\mathbf{A}$. The main advantage regarding the vector potential is its direct relationship with the current density [16]. Indeed, combining the definition of the vector potential

$$\mathbf{B} = \nabla \times \mathbf{A} \tag{3.19}$$

with the Ampère's law

$$\nabla \times \mathbf{B} = \mu_0 \mathbf{J} \tag{3.20}$$

it is possible to write, with the choice of Coulomb gauge ($\nabla \cdot \mathbf{A}$):

$$\nabla^2 \mathbf{A} = -\mu_0 \mathbf{J} \tag{3.21}$$

However, in the case of toroidal system, a three-dimensional description results to be very complicated, since it is necessary to take in account all three components of the vector potential. For this reason it is preferable to apply this procedure only for simplified systems, for example assuming axial symmetry, which determines $\mathbf{A} = A_\phi(\xi, \eta)$ [26]. Considering that the goal of this work is to provide a general description suitable for the majority of the toroidal configurations, we will exclude studies concerning the vector potential.

3.3 Complete expansion in toroidal harmonics

A complete description of the magnetic field generated inside a torus can be obtained adding a supplementary function $M^{\phi}_{0,0}\psi_\phi$ to the general solution of the Laplace's equation *(3.10)*. This is necessary because the considered toroidal geometry represent a doubly connected domain. For this investigation it is preferable to write the expression of the resulting scalar potential in the explicit form displayed in equation *(3.22)*, in order to consider all the possible combinations of sinusoidal and cosinusoidal contributions; the corresponding multipolar moments will be identified with $M^{ij}_{m,n}$, where:

- m is the separation index related to the poloidal periodicity; since the poloidal angle η is a 2π-periodic function, m is defined only with integer

values; this index identifies the order of the multipole moment, in particular, $m = 1$ corresponds to a dipole, $m = 2$ to a quadrupole, $m = 3$ to a sextupole and so on. A solution with $m = 0$ is not realistic, hence the summation can start from $m = 1$;

- n is the separation index associated to the toroidal periodicity of the system and, since also the toroidal angle ϕ is a 2π-periodic function, n takes only integer values. If the placement of the coils determines periodicity of N_T, the allowed values are $n = 0, N_T, 2N_T, ..., N$; $N_T = 1$ corresponds to absence of periodicity;

- i is related to the nature of the components dependent on ϕ which multiply the term $M^{ij}_{m,n}$ present in the summation of the Laplace's solution, in particular $i = c$ if the function depending on ϕ is cosinusoidal, $i = s$ if it is sinusoidal;

- j, similarly, is linked to the nature of the components dependent on η which multiply the term $M^{ij}_{m,n}$; $j = c$ for cosinusoidal components, $j = s$ for sinusoidal components.

$$\psi(\xi,\eta,\phi) = M^{\phi}_{00}\phi + \sqrt{\cosh(\xi)-\cos(\eta)} \sum_{m=1}^{M}\sum_{n=0}^{N} Q^{n}_{m-\frac{1}{2}}(\cosh(\xi)) \left[M^{cc}_{m,n}\cos(n\phi)\cos(m\eta) + M^{cs}_{m,n}\cos(n\phi)\sin(m\eta) + M^{sc}_{m,n}\sin(n\phi)\cos(m\eta) + M^{ss}_{m,n}\sin(n\phi)\sin(m\eta) \right] \quad (3.22)$$

The magnetic field components are deduced applying the gradient to the whole expression of the scalar potential, in toroidal coordinates (see section 1.4.3). Regarding the additional term, it is imposed $\psi_\phi = \phi$; meaning and consequences of this choice are explained below.

$$B_\xi(\xi,\eta,\phi) = \frac{k^{\frac{3}{2}}}{a}\sum_{m=1}^{M}\sum_{n=0}^{N}\Big[M^{cc}_{m,n}\cos(n\phi)\cos(m\eta) + M^{cs}_{m,n}\cos(n\phi)\sin(m\eta) + M^{sc}_{m,n}\sin(n\phi)\cos(m\eta) + M^{ss}_{m,n}\sin(n\phi)\sin(m\eta)\Big] \times \left\{\frac{1}{2}k^{-1}\sinh(\xi)Q^n_{m-\frac{1}{2}}(\cosh(\xi)) + \frac{\partial}{\partial\xi}Q^n_{m-\frac{1}{2}}(\cosh(\xi))\right\} \quad (3.23)$$

$$B_\eta(\xi,\eta,\phi) = \frac{k^{\frac{3}{2}}}{R_p}\sum_{m=1}^{M}\sum_{n=0}^{N}Q^n_{m-\frac{1}{2}}(\cosh(\xi))\Big[\frac{1}{2}\sin(\eta)k^{-1} \times \Big(M^{cc}_{mn}\cos(n\phi)\cos(m\eta) + M^{cs}_{m,n}\cos(n\phi)\sin(m\eta) + M^{sc}_{m,n}\sin(n\phi)\cos(m\eta) + M^{ss}_{m,n}\sin(n\phi)\sin(m\eta)\Big) + m\Big(-M^{cc}_{m,n}\cos(n\phi)\sin(m\eta) + M^{cs}_{m,n}\cos(n\phi)\cos(m\eta) - M^{sc}_{m,n}\sin(n\phi)\sin(m\eta) + M^{ss}_{m,n}\sin(n\phi)\cos(m\eta)\Big)\Big] \quad (3.24)$$

$$B_\phi(\xi,\eta,\phi) = \frac{kM^\phi_{00}}{a\sinh(\xi)} + \frac{k^{\frac{3}{2}}}{a\sinh(\xi)}\sum_{m=1}^{M}\sum_{n=0}^{N}nQ^n_{m-\frac{1}{2}}(\cosh(\xi)) \times \Big[-M^{cc}_{m,n}\sin(n\phi)\cos(m\eta) - M^{cs}_{m,n}\sin(n\phi)\sin(m\eta) + M^{sc}_{m,n}\cos(n\phi)\cos(m\eta) + M^{ss}_{m,n}\cos(n\phi)\sin(m\eta)\Big] \quad (3.25)$$

The additional term $M_{00}^{\phi}\psi_{\phi}$, which can be called *ideal contribute*, represents the magnetic field due to net currents flowing along the z-axis, expressed by:

$$I = \frac{2\,\pi}{\mu_0} M_{00}^{\phi} \tag{3.26}$$

where $\mu_0 = 4\pi \times 10^{-7}$ Henry/m is the permeability of the free space. By choosing $\psi_{\phi} = \phi$, the contribute of magnetic field determined by the supplementary function results to be axisymmetric; combining it with equation *(3.26)* and converting the resulting equation from toroidal to cylindrical coordinates[3], it is clear that the magnetic field due to the additional term is exactly the magnetic field of an ideal torus, which has been deducted in section 1.1, applying the Biot-Savart law.

$$Toroidal\,coordinates:\ B_{\phi} = \frac{k}{a\sinh\xi} M_{00}^{\phi} = \frac{k}{a\sinh\xi}\frac{\mu_0 I}{2\,\pi} \tag{3.28a}$$

$$Cylindrical\,coordinates:\ B_{\phi} = \frac{\mu_0 I}{2\,\pi R} \tag{3.28b}$$

3.4 Possible simplifications

Espression *(3.22)* can be simplified when the studied system presents particular symmetries. Some examples are listed below.

- If the investigation concerns an axisymmetric field, as for example the case of a tokamak, the index n can only be equal to zero. Consequently, the terms $M_{m,0}^{sc}$ and $M_{m,0}^{sc}$ must be held to fixed values, which for simplicity are always choosen equal to zero. This is fundamental to avoid indetermination when we try to evaluate the values of all the coefficients (a procedure with this aim is proposed in the following chapter);
- the system of interest can be also antisymmetric; in a cylindrical coordinate system the antisymmetric condition is expressed by:

[3]The relations between cylindrical (R, θ, z) and toroidal coordinates are:

$$R = a\frac{\sinh\xi}{k},\ z = a\frac{\sin\eta}{k},\ \theta = \phi \Rightarrow \frac{k}{a\sinh\xi} = \frac{1}{R} \tag{3.27}$$

$$\psi(R, \theta, z) = -\psi(R, -\theta, -z) \tag{3.29}$$

This implies that the terms $M^{cc}_{m,n}$, $M^{ss}_{m,n}$ can be chosen equal to zero;

- another possible symmetry is expressed by the relation:

$$\psi(R, \theta, z) = \psi(R, -\theta, -z) \tag{3.30}$$

which allows to neglect the terms $M^{cs}_{m,n}$, $M^{sc}_{m,n}$.

4. Computation of the multipolar moments in toroidal configurations

The purpose of the present chapter is to provide a methodology for the computation of the multipolar moments in toroidal configurations. This procedure will be applied to the expressions of the scalar potential and the magnetic field introduced by *B. Ph. van Milligen* [25], explained in section 3.3. Before proceeding to the description of the method, it is advisable to verify the validity of the studied expressions of the magnetic field components.

Since the goal of this work is the investigation of the toroidal magnetic field in the most general form possible, none of the simplifications mentioned in the previous chapter will be taken into consideration. The only assumption required for this study is the absence of plasma in the system; it would in fact be possible to include a zone containing the plasma in the description: this contribute can be represented by a summation very similar to the one introduced in *(3.22)*, but in this case it involves the associated Legendre functions with half-integer indexes of the first kind, $P^n_{m-\frac{1}{2}}(\cosh(\xi))$; moreover, a supplementary term is necessary to describe the magnetic field caused by the line current induced by the plasma, along the reference radius of the torus [25].

4.1 Verification of the magnetic field expressions

One of the critical aspects of this investigation is the presence of the associated Legendre functions with half-integer indexes, which are dependent on the coordinate ξ and on the indexes n, m. Their trend is not easy to evaluate and understand, as discussed in chapter 3, therefore it is advisable to verify the

expressions obtained for the magnetic field, which involve the mentioned Legendre functions. This validation can be performed by implementing equation *(3.23)*, *(3.24)* and *(3.25)* on MATLAB in order to plot the vectors of the magnetic field and make considerations about simple expected properties.

4.1.1 Definition of the toroidal grid

For the verification, a three-dimensional toroidal grid of $N_r \times N_\theta \times N_\phi = 21 \times 21 \times 21 = 9261$ points has been defined. The set (r, θ, ϕ) corresponds to the elementary toroidal coordinate system described in section 1.3; it is important to underline that this coordinate system was used only for the definition of the toroidal grid, subsequently these points were converted in Cartesian coordinates and, lastly, in the most suitable toroidal coordinate set introduced in section 1.4.2. The latter conversion is fundamental for the implementation of the magnetic field formulas obtained from the scalar potential expansion, which indeed has been obtained in toroidal coordinates.

A relevant parameter for the definition of a toroidal geometry is the so called *effect of curvature* ε, specified by the relation:

$$\varepsilon = \frac{r}{R_0} \tag{4.1}$$

where r is the minor radius and R_0 is the major radius of the torus, as displayed in *Figure 4.1.*

This parameter quantifies the distortion of the magnetic field generated by a toroidal magnet with respect to the *straight cylindrical magnet of origin.* Indeed, as explained in chapter 1.4.3, toroids can be seen as solenoids bent into the shape of a circle. The main consequence of this curvature, concerning with the magnetic field, is the loss of symmetry with respect to the axis inside the magnet. A decrease of ε corresponds to a movement of the pole to the center of the toroidal section, which is reached when $\varepsilon = 0$. A typical value of this parameter is $\varepsilon = 0.5$, which can be obtained for example choosing $r = 0.5$ m and $R_0 = 1$ m [26].

Figure 4.2 and *Figure 4.3* show the resulting toroidal grid seen in section on the $xz - plane$ and on the $xy - plane$, respectively.

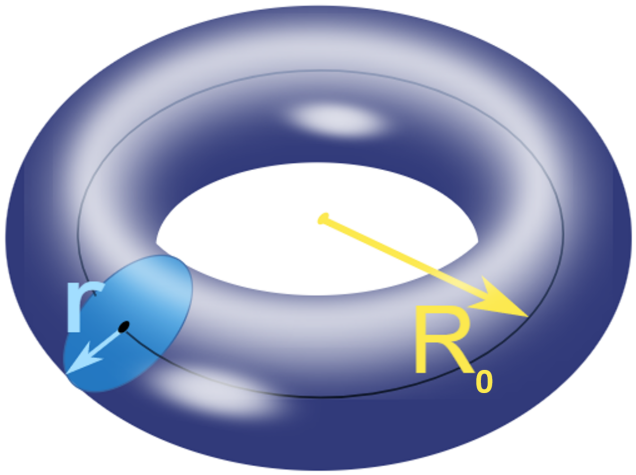

Figure 4.1 Representation of the minor (light blue) and major (yellow) radius of a generic torus.

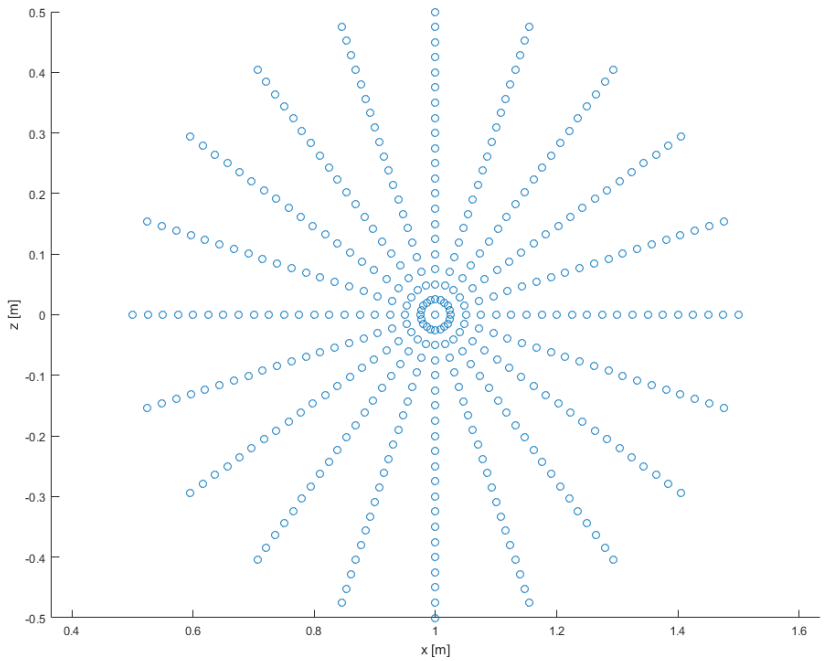

Figure 4.2 Toroidal grid on the $xz - plane$.

4.1.2 Verified magnetic fields

For the evaluation of the magnetic field on the defined grid, it is necessary to choose values of the indexes n and m and of each multipolar moment $M^{ij}_{m,n}$. As

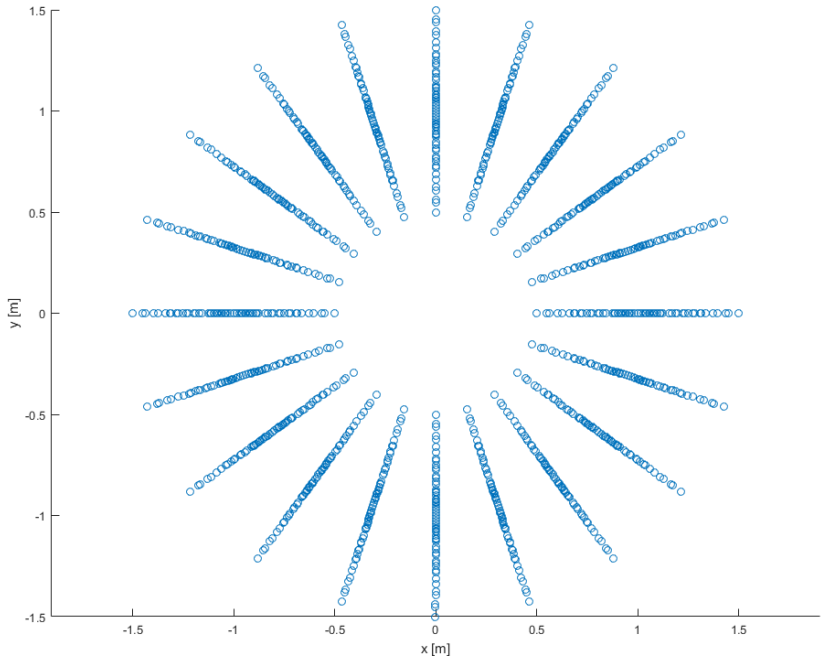

Figure 4.3 Toroidal grid on the $xy - plane$.

explained in section 3.3, the term M_{00}^{ϕ} represents the ideal magnetic field contribute, which is axisymmetric (with respect of the $z - axis$), presents a magnitude that decreases when the distance from $z - axis$ increases and has concentric field lines, closed on themselves. This trend is expected when the term M_{00}^{ϕ} is dominant compared to the other multipole coefficients and $n = 0$; if these two conditions are verified, the value of the index m is not relevant for the description of the magnetic field. It is possible to verify this trend imposing the values of *Table* 4.1; the resulting magnetic field has the expected trend, as shown in *Figure 4.4* and in *Figure 4.5*, which display a global and a particular view of the vectors of the magnetic field on the $xy - plane$, respectively. It is important to highlight that is a discretized representation of th magnetic field components, which are represented only for the finite number of points defined by the considered toroidal grid. This decision was made in order to have a clearer representation, although is known that the the magnetic field lines cover the whole volume of the torus, describing circumferences closed on themselves.

A relevant result can be obtained setting the values displayed in *Table* 4.2. Indeed, one can expect that the the necessary and sufficient condition to have

Index or coefficient	Value
n	0
m	1
M_{00}^{ϕ}	100
$M_{m,n}^{cc}$	1
$M_{m,n}^{cs}$	1
$M_{m,n}^{sc}$	1
$M_{m,n}^{ss}$	1

Table 4.1 Values of multipolar coefficients corresponding to an ideal magnetic field.

an ideal toroidal field is the choice of $n = 0$, which correspond to absence of toroidal periodicity. However, as can be seen in *Figure 4.6*, the only condition of absence of periodicity is not sufficient to obtain the ideal toroidal field: the resulting magnetic field is axisymmetric but the field lines are not concentric and closed on themselves, as they were in the ideal case shown in *Figure 4.4*.

Index or coefficient	Value
n	0
m	1
M_{00}^{ϕ}	1
$M_{m,n}^{cc}$	1
$M_{m,n}^{cs}$	1
$M_{m,n}^{sc}$	1
$M_{m,n}^{ss}$	1

Table 4.2 Values imposed to prove the insufficiency of the only condition $n = 0$ for the definition of an ideal magnetic field.

No further verifications are described, as they are not relevant for the purposes of the analysis. If the values of the indexes n and m are modified, we

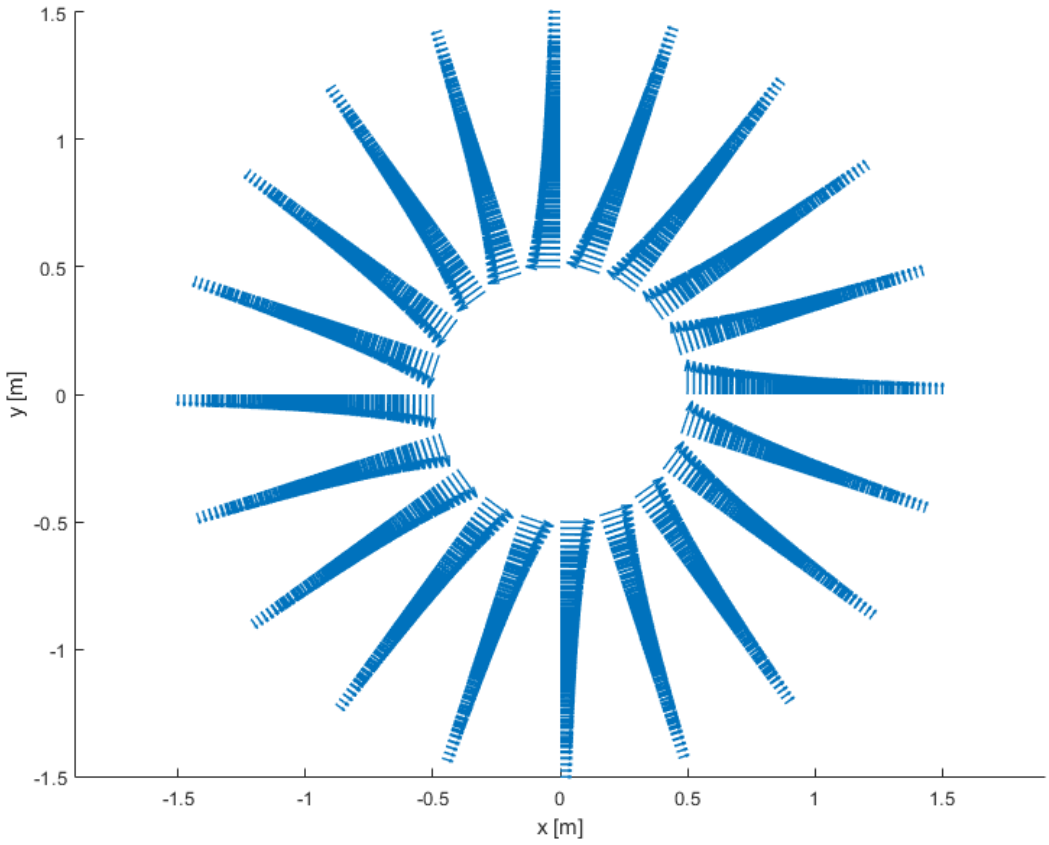

Figure 4.4 Global representation on the $xy - plane$ of the vectors of the ideal magnetic field obtained setting the values of *Table 4.1*.

expect fluctuations of the magnetic field vectors with respect to the previous cases. Unfortunately, the complex form of the expressions of the magnetic field components does not allow an intuitive identification of the individual contributions of the moments and of the periodicity of the system.

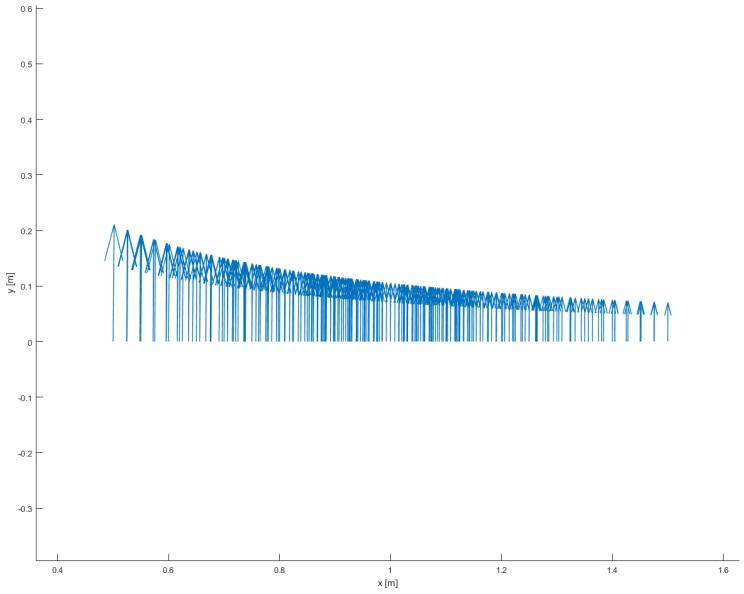

Figure 4.5 Particular representation on the $xy-plane$ of the vectors of the ideal magnetic field obtained setting the values of *Table 4.1*.

4.2 Evaluation of multipolar moments

We have developed a tool for the determination of the multipolar moments. With this tool it is possible to identify the dominant harmonics of a specified toroidal magnet. The requirement for the application of this procedure is the knowledge of the magnetic field at a fixed radial coordinate $\xi = \xi_0$, for L values of the poloidal angle η and S values of the toroidal angle ϕ. This request can be satisfied evaluating numerically the magnetic field (employing the Biot-Savart law) or measuring it, for example by means of rotating induction coils [14]. Theoretically, the multipolar moments can be determined both from the magnetic field and the scalar potential; however, for this analysis it is preferable to work with the scalar potential, due to the complicated analytical expressions of the magnetic field.

Fixed the value $\xi = \xi_0$ and chosen one of the S angles $\phi = \phi_s$, the only variable left is η, hence the scalar potential can be written as:

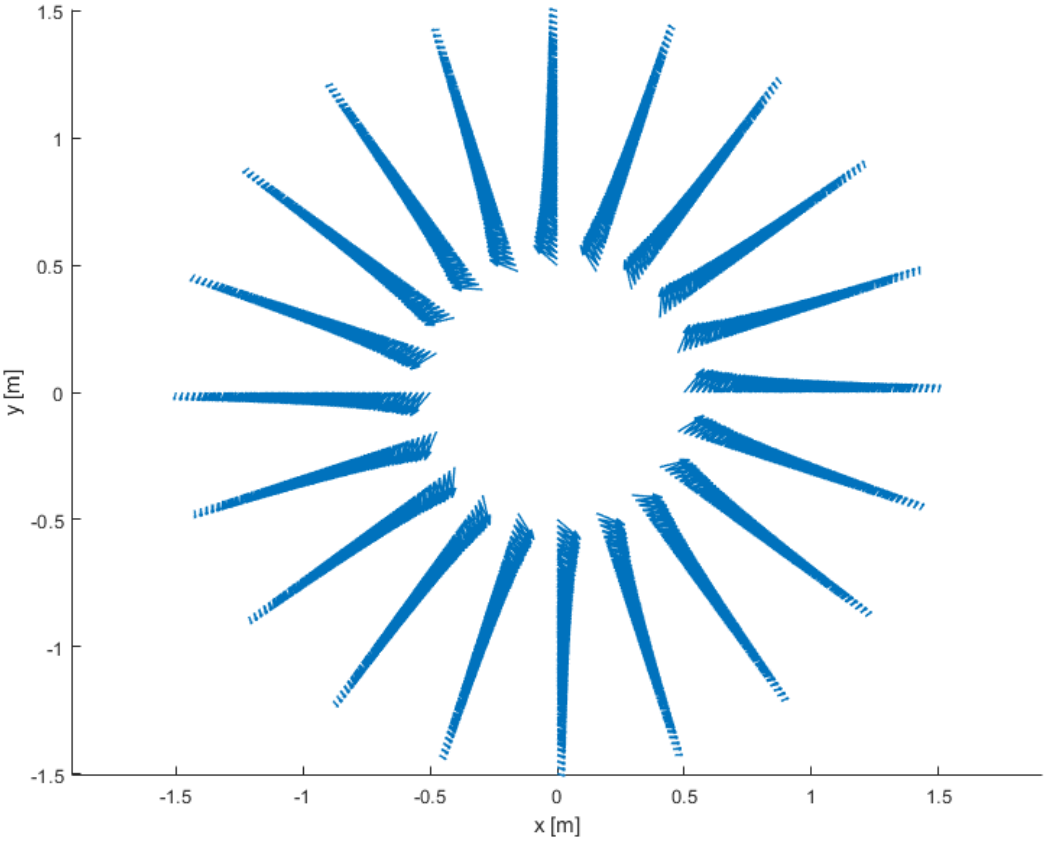

Figure 4.6 Vectors of the magnetic field corresponding to values of *Table* 4.2.

$$\psi(\xi_0,\eta,\phi_s) = M_{00}^{\phi}\phi_s + \sqrt{\cosh(\xi_0)-\cos(\eta)}\sum_{m=1}^{M}\sum_{n=0}^{N} Q_{m-\frac{1}{2}}^{n}(\cosh(\xi_0))$$
$$\Big[M_{m,n}^{cc}\cos(n\phi_s)\cos(m\eta) + M_{m,n}^{cs}\cos(n\phi_s)\sin(m\eta)$$
$$+ M_{m,n}^{sc}\sin(n\phi_s)\cos(m\eta) + M_{m,n}^{ss}\sin(n\phi_s)\sin(m\eta)\Big] \quad (4.2)$$

Since many of the terms of this expression are constant, we can manipulate it in order to have in evidence the variable contributions, which depend on η.

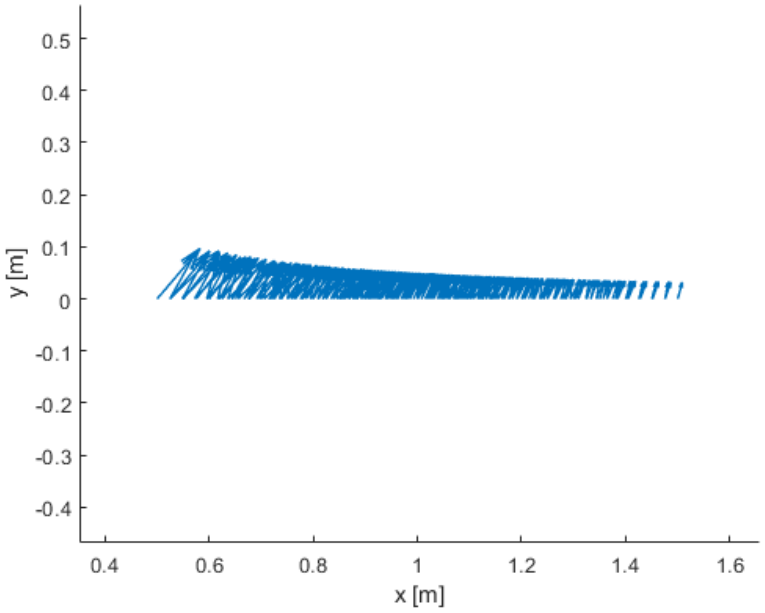

Figure 4.7 Particular representation on the $xy-plane$ of the vectors of the ideal magnetic field obtained setting the values of *Table 4.2*.

$$\psi(\xi_0,\eta,\phi_s) = M_{00}^{\phi}\phi_s + \sqrt{\cosh(\xi_0)-\cos(\eta)} \times \sum_{m=1}^{M}\sum_{n=0}^{N}\Big\{ Q^n_{m-\frac{1}{2}}(\cosh(\xi_0))\Big[M^{cc}_{m,n}\cos(n\phi_s) + M^{sc}_{m,n}\sin(n\phi_s)\Big]\cos(m\eta) + Q^n_{m-\frac{1}{2}}(\cosh(\xi_0))\Big[M^{cs}_{m,n}\cos(n\phi_s) + M^{ss}_{m,n}\sin(n\phi_s)\Big]\sin(m\eta)\Big\} \quad (4.3)$$

Equation *(4.3)* can also be written as follow.

$$\psi(\xi_0,\eta,\phi_s) = M_{00}^{\phi}\phi_s + \sqrt{\cosh(\xi_0)-\cos(\eta)} \times \Big\{ \sum_{m=1}^{M}\sum_{n=0}^{N} Q^n_{m-\frac{1}{2}}(\cosh(\xi_0))\Big[M^{cc}_{m,n}\cos(n\phi_s) + M^{sc}_{m,n}\sin(n\phi_s)\Big]\cos(m\eta) + \sum_{m=1}^{M}\sum_{n=0}^{N} Q^n_{m-\frac{1}{2}}(\cosh(\xi_0))\Big[M^{cs}_{m,n}\cos(n\phi_s) + M^{ss}_{m,n}\sin(n\phi_s)\Big]\sin(m\eta)\Big\} \quad (4.4)$$

The constant terms multiplying $\cos(m\eta)$ and $\sin(m\eta)$ will be identified as $A_m(\xi_0, \phi_s)$ and $B_m(\xi_0, \phi_s)$, respectively. It is worth to underline that these terms are constant only when specific values of ξ and ϕ are chosen.

$$A_m(\xi_0, \phi_s) = \sum_{n=0}^{N} Q^n_{m-\frac{1}{2}}(\cosh(\xi_0))\Big[M^{cc}_{m,n}\cos(n\phi_s) + M^{sc}_{m,n}\sin(n\phi_s)\Big] \tag{4.5a}$$

$$B_m(\xi_0, \phi_s) = \sum_{n=0}^{N} Q^n_{m-\frac{1}{2}}(\cosh(\xi_0))\Big[M^{cs}_{m,n}\cos(n\phi_s) + M^{ss}_{m,n}\sin(n\phi_s)\Big] \tag{4.5b}$$

Consequently, equation *(4.4)* can be written in the form:

$$\psi(\xi_0, \eta, \phi_s) = M^{\phi}_{00}\phi_s + \sqrt{\cosh(\xi_0) - \cos(\eta)} \times \sum_{m=1}^{M}\Big(A_m(\xi_0, \phi_s)\cos(m\eta) + B_m(\xi_0, \phi_s)\sin(m\eta)\Big) \tag{4.6}$$

The expression obtained varies only with η and describes the scalar potential at a fixed radius (identified by ξ_0) and at a fixed toroidal angle (identified by ϕ_s). The coefficients M^{ϕ}_{00}, A_m and B_m are still to be determined. For a specific toroidal magnet, whose scalar potential is known at a given number of points, the mentioned coefficients can be determined employing a fitting procedure. The method, which will be called *Fitting 1*, can be described schematically as follows.

FITTING 1

- **Input** $\rightarrow$ Values of the scalar potential, measured or numerically evaluated at $\xi = \xi_0$, $\phi = \phi_s$ for L equidistant values of η, whose placement is determined by the relation:

$$\eta_l = \frac{2\pi l}{L}$$

where $l = 0, 1, ..., L-1$.

- **Fitting equation** → Equation *(4.6)*:

$$\psi(\xi_0, \eta, \phi_s) = M_{00}^{\phi}\phi_s + \sqrt{\cosh(\xi_0) - \cos(\eta)} \sum_{n=0}^{N} \Big(A_m(\xi_0, \phi_s)\cos(m\eta) + B_m(\xi_0, \phi_s)\sin(m\eta) \Big)$$

- **Output** → Coefficients M_{00}^{ϕ}, $A_m(\xi_0, \phi_s)$ and $B_m(\xi_0, \phi_s)$.

At the end of this first procedure of fitting, only the coefficient related to the ideal contribute of the magnetic field M_{00}^{ϕ} is actually known; the effective values of the specific multipolar components are undetermined at this stage. Indeed, the terms A_m and B_m involve many contributions of the toroidal harmonics, which need to be distinguished. For this purpose, it is necessary to apply all the steps described so far a to a different value of $\phi = \phi_{s'}$, obtaining new results A' and B'; the coefficient $M'^{\,\phi}_{00}$ is expected to be equal to the coefficient M_{00}^{ϕ} of the previous calculation, hence it can be identified with the notation M_{00}^{ϕ} for any ϕ. This procedure is repeated for S angles ϕ, whose placement is defined by the relation:

$$\phi_s = \frac{2\pi s}{S}$$

where $s = 0, 1, ..., S-1$.

The result of this last step is a set of S values of A_m and a set of S values of B_m, which depend on the angle ϕ and on the fixed value ξ_0. These data can be interpreted as the *known data* of the previous fitting; therefore it is possible to employ a similar method to fit them and obtain the coefficients $M_{m,n}^{cc}$, $M_{m,n}^{sc}$, $M_{m,n}^{cs}$, $M_{m,n}^{ss}$, for each value of n and m. The procedures implemented will be called *Fitting 2A* and *Fitting 2B*; they are schematically described below.

FITTING 2A

- **Input** → Values of A_m evaluated at $\xi = \xi_0$ for S equidistant angles ϕ, whose placement is defined by the relation:

$$\phi_s = \frac{2\pi s}{S}$$

where $s = 0, 1, ..., S-1$.

- **Fitting equation** → Equation *(4.5a)* written with the coordinate ϕ variable and not fixed:

$$A_m(\xi_0, \phi) = \sum_{n=0}^{N} Q^n_{m-\frac{1}{2}}(\cosh(\xi_0))\Big[M^{cc}_{m,n}\cos(n\phi) + M^{sc}_{m,n}\sin(n\phi)\Big]$$

- **Output** → Coefficients $M^{cc}_{m,n}$, $M^{sc}_{m,n}$.

FITTING 2B

- **Input** → Values of B_m evaluated at $\xi = \xi_0$ for S equidistant angles ϕ, whose placement is defined by the relation:

$$\phi_s = \frac{2\pi s}{S}$$

where $s = 0, 1, ..., S-1$.

.

- **Fitting equation** → Equation *(4.5b)* written with the coordinate ϕ variable and not fixed:

$$B_m(\xi_0, \phi) = \sum_{n=0}^{N} Q^n_{m-\frac{1}{2}}(\cosh(\xi_0))\Big[M^{cs}_{m,n}\cos(n\phi) + M^{ss}_{m,n}\sin(n\phi)\Big]$$

- **Output** → Coefficients $M^{cs}_{m,n}$, $M^{ss}_{m,n}$.

At the end of the three fitting procedures, the values of each coefficient, introduced in the multipolar expansion of the scalar potential, are known. These terms can also be substituted in the expression of the magnetic field components *(3.23)*, *(3.24)*, *(3.25)*. Therefore, employing the described technique, the most relevant multipoles of a specific toroid can be identified. Moreover, it is possible to find the values of the scalar potential and each component of the magnetic field, for a given surface with fixed $\xi = \xi_0$ and for any values of η and ϕ.

4.2.1 Verification of the fitting procedure

A simple strategy to verify the validity of the described procedure consists of choosing values for each coefficient M^{ϕ}_{00} and $M^{ij}_{m,n}$ and considering the corresponding scalar potential as the *known potential*, required for the

application of the method. The chosen values will be called $\widetilde{M}^{ij}_{m,n}$, $\widetilde{M}^{\phi}_{00}$; the corresponding scalar potential, shown in equation *(4.7)*, is calculated at a fixed ξ_0, for S angles ϕ and L angles η.

$$\widetilde{\psi}(\xi_0,\eta,\phi) = \widetilde{M}^{\phi}_{00}\phi + \sqrt{\cosh(\xi_0)-\cos(\eta)}\sum_{m=1}^{M}\sum_{n=0}^{N} Q^{n}_{m-\frac{1}{2}}(\cosh(\xi_0)) \left[\widetilde{M}^{cc}_{m,n}\cos(n\phi)\cos(m\eta) + \widetilde{M}^{cs}_{m,n}\cos(n\phi)\sin(m\eta) + \widetilde{M}^{sc}_{m,n}\sin(n\phi)\cos(m\eta) + \widetilde{M}^{ss}_{m,n}\sin(n\phi)\sin(m\eta)\right] \quad (4.7)$$

All the steps of the described procedure are followed; the resulting multipolar moments $M^{ij}_{m,n}$ and M^{ϕ}_{00} should be equal to the multipolar moments chosen for the known potential, $\widetilde{M}^{ij}_{m,n}$, $\widetilde{M}^{\phi}_{00}$. It is important to underline that, for this verification, the value $\phi = 0$ must be excluded. Indeed this choice would imply indetermination in the evaluation of the correspondent coefficient M^{ϕ}_{00}: the term $\widetilde{M}^{\phi}_{00}$ of the known scalar potential can assume any values, when $\phi = 0$. A reasonable solution to this problem is the choice of $\frac{2\pi}{S}$ as the first value of the angle ϕ. Following the development of various analyzes, in which indexes and coefficients have been changed, it is possible to conclude that the described fitting procedure is satisfactory for the computation of the multipolar moments. The results of one example of verification is displayed in *Table 4.2.1.* For the purpose of simplicity, the reported example presents only one value of the index m and two values of the index n, in particular $n = 0, 8$ and $m = 1$. ξ_0 is chosen equal to 2.333.

Multipolar coefficients	**Difference**	**Percentage error** [%]
$\widetilde{M}^{\phi}_{00} - M^{\phi}_{00}$	-3.08×10^{-6}	0
$\widetilde{M}^{cc}_{1,0} - M^{cc}_{1,0}$	-3.08×10^{-9}	-0.0549
$\widetilde{M}^{cs}_{1,0} - M^{cs}_{1,0}$	-1.28×10^{-4}	-0.0549
$\widetilde{M}^{cc}_{1,8} - M^{cc}_{1,8}$	-2.29×10^{-6}	-0.0002
$\widetilde{M}^{cs}_{1,8} - M^{cs}_{1,8}$	-6.55×10^{-6}	-0.0002
$\widetilde{M}^{sc}_{1,8} - M^{sc}_{1,8}$	-5.31×10^{-7}	-0.0002
$\widetilde{M}^{ss}_{1,8} - M^{ss}_{1,8}$	-6.19×10^{-7}	-0.0002

Table 4.3 Example of the verification of the fitting procedure.

5. Results and discussion

In the first part of this chapter, a possible method for the numerical calculation of the scalar potential is proposed. The computation of the scalar potential, on a defined three-dimensional grid of points, is a requirement for the employment of the fitting procedure described in the previous chapter. This will be accomplished using *Field 2017*, a computational tool developed by *Jeroen van Nugteren* [27]. After a brief description of the choice made for the computation, the results obtained from the fitting procedure application will be presented and discussed.

5.1 Numerical evaluation of the scalar potential

The initial step for the calculation of the scalar potential is the definition of the toroidal configuration. The mentioned computational tool allows one customizing the system from many points of view; some of them are listed below.

- The type of magnet, which in this case will be a toroid;
- the size, the shape and the number of the coils; for simplicity we will consider regular circular coils, whose number will vary depending on the kind on analysis requested; for what concern the size, in order to have the effect of curvature $\varepsilon = 0.5$, as proposed in chapter 4, we set the minor radius of the torus equal to 0.5 m and the major radius of the torus equal to 1 m;
- the number of pancake of each coil: in this computation we will consider coils consisting in only one pancake each;
- the current flowing in each pancake, that in the first instance will be chosen equal to 1 kA and then some consideration about cases with current 5 kA will be presented.

Once established the toroidal system, it is necessary to define the grid on which to compute the magnetic field. After several verifications, it has been concluded that the best solution is to define a cylindrical grid, concentric to the toroid. This choice is linked to the requirements of some functions, which will be implemented during the procedure. The major radius of the cylindrical grid has been chosen slightly smaller than the outermost radius of the torus, in order to avoid the board effects caused by the coils.

Subsequently, it is necessary to convert the points of the cylindrical grid in Cartesian coordinates, because *Field 2017* evaluates the Cartesian components of the magnetic field: B_x, B_y and B_z.

Since it is not possible to calculate analytically the scalar potential with a simple integration of the magnetic field components, it is necessary to employ a numerical integration [28].

5.1.1 Verification of the integration process

To verify the validity of this integration process, a possible strategy is to apply the gradient to the obtained scalar potential. The resulting magnetic field components, known on each point of the defined grid, can be represented and compared with the magnetic field components computed by *Field 2017*. After several verifications, we can conclude that the method is satisfactory; for completeness an example is provided.

Figure 5.1 and *Figure 5.2* show the vectors of the magnetic field provided by the software and calculated from the scalar potential, respectively; both of them are evaluated in a portion of the torus characterized by $0 < \phi < \pi/4$. The parameters which characterize the reported example are the same as those used for *Case 1* of section 5.2.

5.1.2 Scalar potential on the reference points

Once established that the methodology is satisfactory, it is possible to proceed with the evaluation of the scalar potential on the specific points necessary for the fitting procedure. Based on how the toroidal geometry was defined, an appropriate value of ξ_0 results to be 2.333. Indeed, the coordinate surface corresponding to this value is placed in an intermediate area of the toroid, far enough from the coils. This is essential, because close to the coils the magnetic

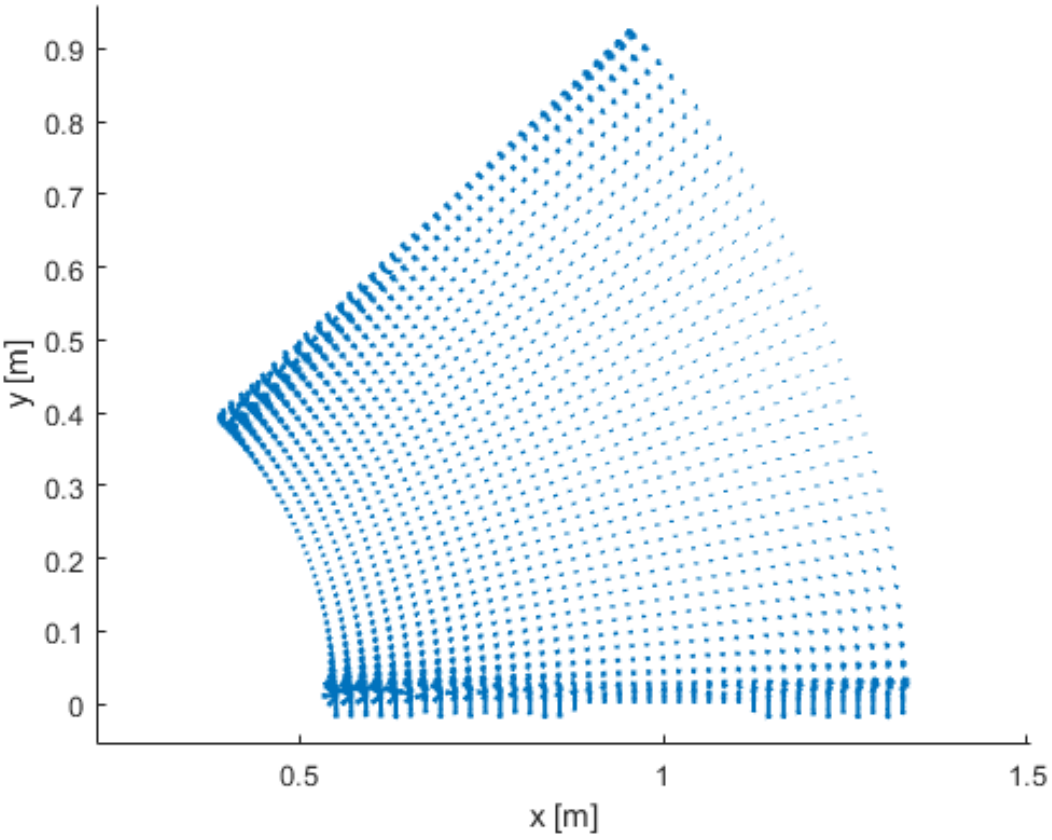

Figure 5.1 Vectors of magnetic field provided by *Field 2017*, on $xy-plane$, for a portion of torus $0 < \phi < \pi/4$.

field and the scalar potential can exhibit errors and strong fluctuations. For a toroid with effect of curvature $\varepsilon = 0.5$, the extreme values of ξ are $\xi_{max} = 4.673$ and $\xi_{min} = 1.313$. The coordinate surface corresponding to these values of ξ are shown in *Figure 5.3*. As it can be noticed, the points represented in this figure are not equispaced. This is because they were defined in toroidal coordinates and then converted to Cartesian coordinates, in order to be able to plot them with MATLAB.

Regarding the choice of L, which identifies the number of angles η involved in the fitting procedure, a recommended value is 60: it has been proved that this choice allows one to evaluate the multipolar coefficients with sufficient precision up to high multipole orders [14]. For what concern S, that identifies the number of angles ϕ, after several verifications it has been possible to conclude that an

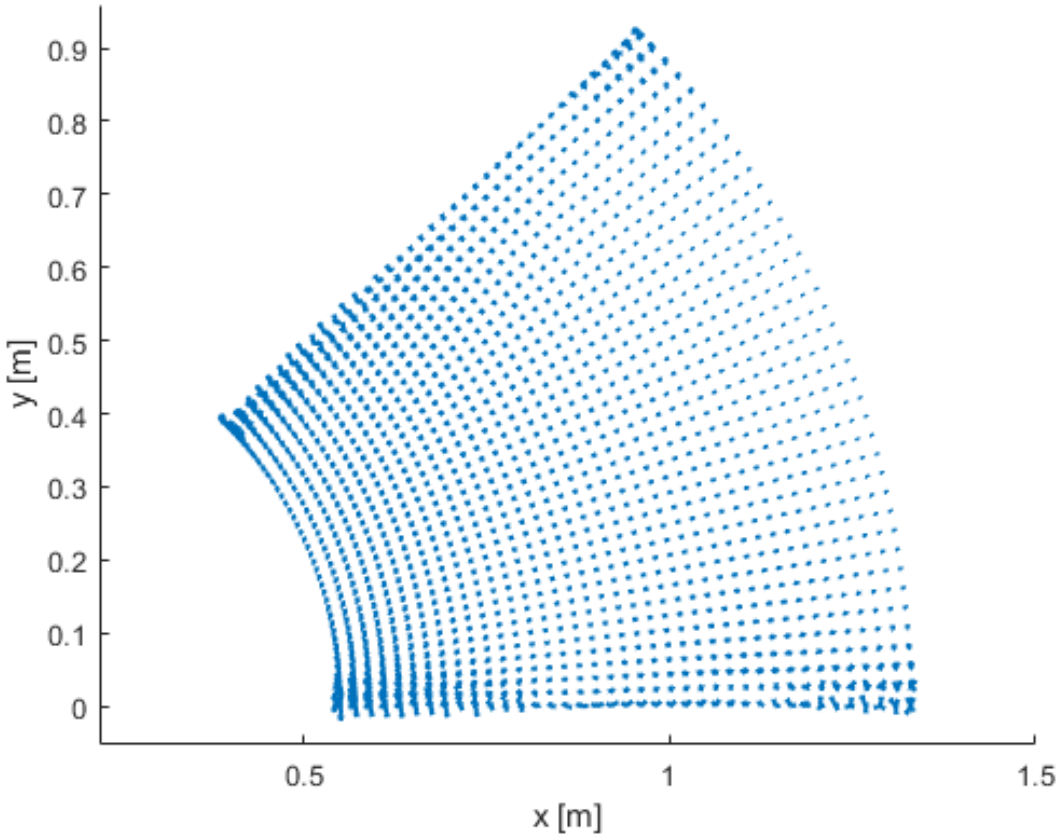

Figure 5.2 Vectors of magnetic field calculated from the scalar potential, on $xy - plane$, for a portion of torus $0 < \phi < \pi/4$.

appropriate value is 40.

5.2 Results

Once evaluated the scalar potential on the reference points, which corresponds to what we called *known scalar potential* in chapter 4, it is possible to apply the fitting procedure. Several cases have been analyzed.

It is important to highlight that the coefficients M^{sc} and M^{ss} are excluded from the computation when $n = 0$, for any value of m. Indeed, as mentioned in section 3.4, these terms are multiplied by

$$\sin(n\phi) = \sin(0) = 0$$

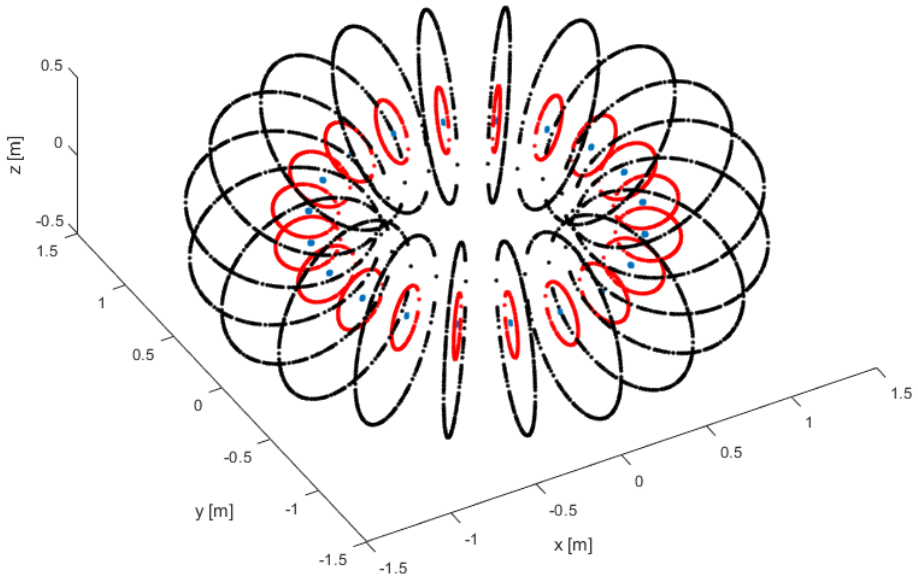

Figure 5.3 Surfaces at $\xi = 4.673$ (black), $\xi = 2.333$ (red) and $\xi = 1.313$ (blue).

hence they would be undeterminate during the computation.

Toroid with 8 coils

The first system analyzed involves a toroid made of 8 coils, shown in *Figure 5.4*. The multipolar components are computed considering different values of the indexes n, m and on different portion of the torus.

- *Case 1*
  Portion of the torus: $0 < \phi < \pi/4$.
  Toroidal index: $n = 0, 8, 16$.
  Poloidal index: $m = 1, 2, 3$.
  Current of each pancake: 1 kA.
  $M_{00}^{\phi} = -0.505$

- *Case 2*
  Portion of the torus: $0 < \phi < \pi/8$.

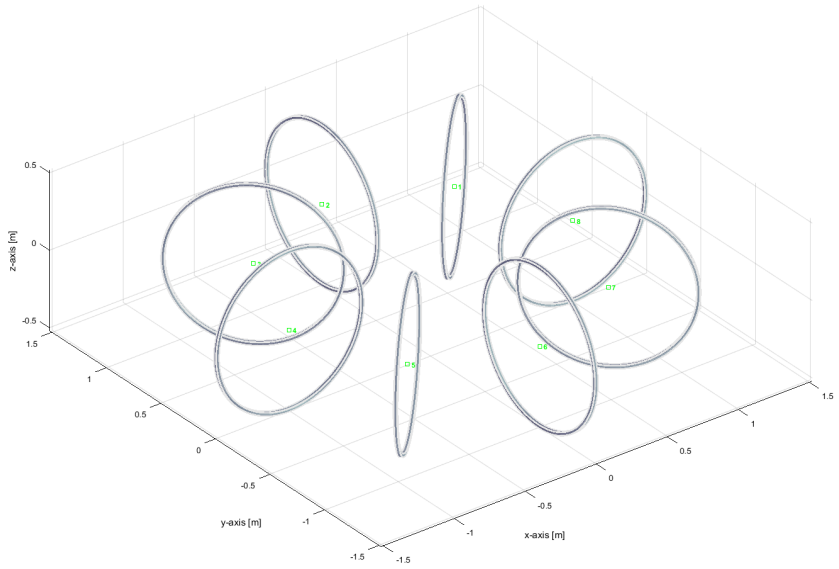

Figure 5.4 Representation of a toroid made of 8 circular coils.

m	**n**	M^{cc}	M^{cs}	M^{sc}	M^{ss}
1	0	0.507	0	–	–
1	8	0	0	1.4×10^{-6}	0
1	16	0	0	0	0
2	0	0.948	0	–	–
2	8	0	0	0	0
2	16	0	0	0	0
3	0	0	0	–	–
3	8	0	0	0	0
3	16	0	0	–	–

Table 5.1 Multipolar moments obtained in *Case 1.*

Toroidal index: $n = 0, 8, 16$.
Poloidal index: $m = 1, 2, 3$.
Current of each pancake: 1 kA.

$M_{00}^{\phi} = -1.393$

m	**n**	M^{cc}	M^{cs}	M^{sc}	M^{ss}
1	0	0.237	0	–	–
1	8	-4.1×10^{-6}	0	0	0
1	16	0	0	0	0
2	0	-4.6×10^{-5}	0	–	–
2	8	0	0	0	0
2	16	0	0	0	0
3	0	0	0	–	–
3	8	0	0	0	0
3	16	0	0	–	–

Table 5.2 Multipolar moments obtained in *Case 2*.

- *Case 3*
  Portion of the torus: $0 < \phi < \pi/16$.
  Toroidal index: $n = 0, 8, 16$.
  Poloidal index: $m = 1, 2, 3$.
  Current of each pancake: 1 kA.
  $M^{\phi}_{00} = -2.670$

m	**n**	M^{cc}	M^{cs}	M^{sc}	M^{ss}
1	0	0	0	–	–
1	8	0	0	0	0
1	16	0	0	0	0
2	0	0	0	–	–
2	8	0	0	0	0
2	16	0	0	0	0
3	0	0	0	–	–
3	8	0	0	0	0
3	16	0	0	–	–

Table 5.3 Multipolar moments obtained in *Case 3*.

- *Case 4*

Portion of the torus: $0 < \phi < \pi/4$.
Toroidal index: $n = 0, 8, 16$.
Poloidal index: $m = 1, 2, 3$.
Current of each pancake: 5 kA.

$M_{00}^{\phi} = -2.524$

m	**n**	M^{cc}	M^{cs}	M^{sc}	M^{ss}
1	0	2.536	0	–	–
1	8	0	0	0	0
1	16	0	0	0	0
2	0	4.741	−0.002	–	–
2	8	0	0	0	0
2	16	0	0	0	0
3	0	0	0	–	–
3	8	0	0	0	0
3	16	0	0	–	–

Table 5.4 Multipolar moments obtained in *Case 4*.

Toroid with 50 coils

The second relevant system analyzed consists of a toroid made of 50 coils, displayed in *Figure 5.5*.

- *Case 5*
  Portion of the torus: $0 < \phi < 2\pi$.
  Toroidal index: $n = 0, 50, 100$.
  Poloidal index: $m = 1, 2, 3$.
  Current of each pancake: 1 kA.

  $M_{00}^{\phi} = 0.119$

- *Case 6*
  Portion of the torus: $0 < \phi < 2\pi$.
  Toroidal index: $n = 0, 50, 100$.

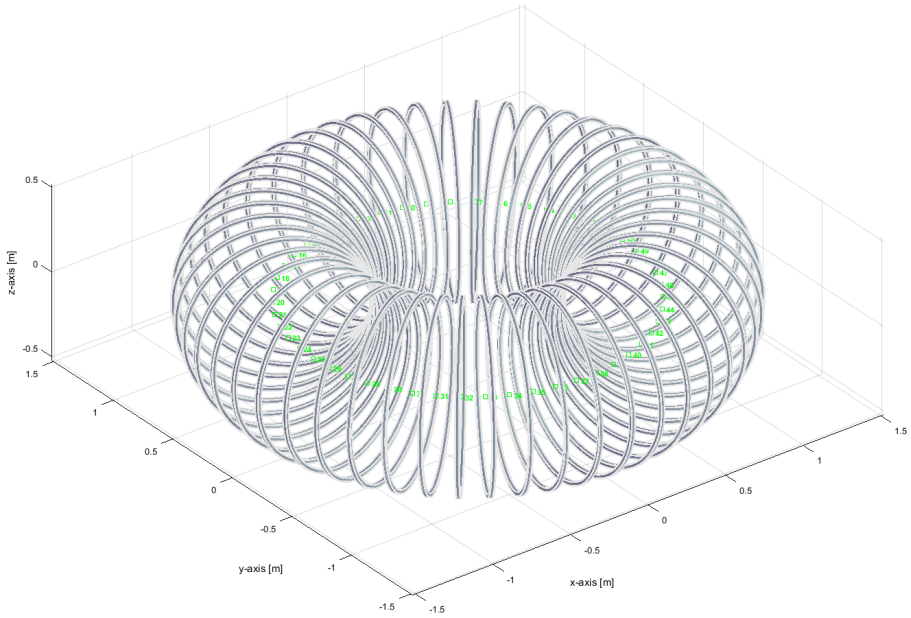

Figure 5.5 Representation of a toroid made of 50 circular coils.

m	**n**	M^{cc}	M^{cs}	M^{sc}	M^{ss}
1	0	0	0	–	–
1	50	0	0	0	0
1	100	0	0	0	0
2	0	0	0	–	–
2	50	0	0	0	0
2	100	0	0	0	0
3	0	0	0	–	–
3	50	0	0	0	0
3	100	0	0	–	–

Table 5.5 Multipolar moments obtained in *Case 5*.

Poloidal index: $m = 1, 2, 3$.
Current of each pancake: 5 kA.

$M_{00}^{\phi} = 0.598$

m	**n**	M^{cc}	M^{cs}	M^{sc}	M^{ss}
1	0	0	0	–	–
1	50	0	0	0	0
1	100	0	0	0	0
2	0	0	0	–	–
2	50	0	0	0	0
2	100	0	0	0	0
3	0	0	0	–	–
3	50	0	0	0	0
3	100	0	0	–	–

Table 5.6 Multipolar moments obtained in *Case 6*.

5.3 Considerations and future studies

The first important consideration about the results obtained regards the portion of torus taken into account for the computation. An appropriate choice of the range of ϕ is decisive for the correctness of the computed multipolar moments. Although it may be thought that, reducing the torus portion, it is possible to have a more precise description, with the same computational effort (i. e. the same S and L), this choice can lead to incomplete results. Comparing the *Cases* $1, 2$ and 3, we can note that reducing the range of ϕ, the ideal component M_{00}^{ϕ} is more and more dominant than the other multipolar components. Since we are analyzing a real magnet with a finite number of coils, we expect to find some discrepancies with respect to the ideal case described in section 1.1. Therefore, if we concentrate our study on a too small area, the distance from the coils determines a loss of information on the mentioned deviations. For this reason, in the case of toroid made of 8 coils, an appropriate range for the evaluation of the multipolar moments is $0 < \phi < \pi/4$.

Although the described procedure can be theoretically employed for infinite values of the indexes n and m, it is reasonable to choose $m = 1$, $m = 2$, $m = 3$ for the poloidal index and $n = 0, N_t$ for the toroidal index. Indeed, as these indexes increase, the corresponding multipolar moments become smaller and smaller, until they are negligible.

Analyzing *Case* 5, we can state that a toroid consisting of 50 coils can be considered as an ideal torus. This is evident in *Figure 5.6*: the vectors of the magnetic field represented in this figure were obtained by replacing in the expressions of the field components, described in chapter 3, the values of the calculated multipolar moments.

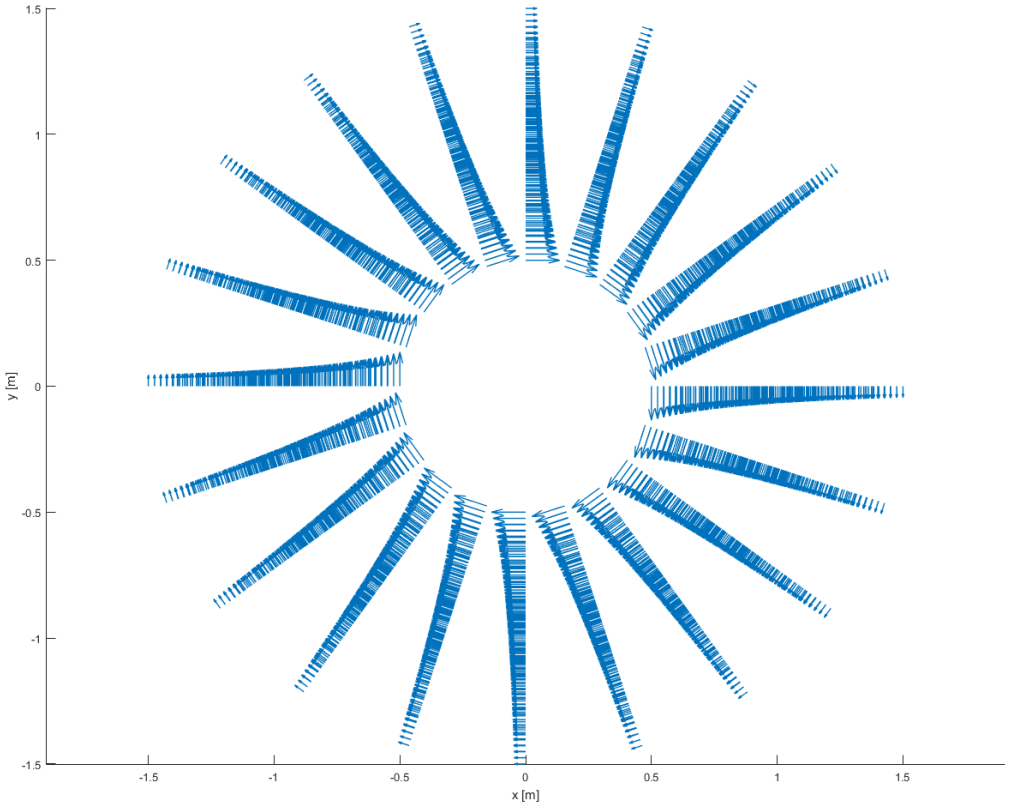

Figure 5.6 Vectors of magnetic field obtained from the evaluated multipolar moments in *Case* 5.

In *Cases* 4 and 6, the current was set to 5 kA. The corresponding multipolar moments have different values compared to cases in which the current is set to 1 kA. It is known that the multipole coefficients are related to the amount of current, but most of the analyzes looking for this link, involve the vector potential instead of the scalar potential [20]. Future studies will investigate the relation between the current and the multipolar moments, evaluated from the

scalar potential.

The developed procedure allows us to evaluate, with satisfactory precision and computational effort, the multipole moments of toroidal systems made of any number of coils.

The possibility of identifying the dominant multipoles is extremely useful in practical applications of magnets, especially in the field of beam optics. Indeed, in the case of straight cylindrical magnets, each kind of multipole has a specific effect: the dipole is used for beam steering, the quadrupole for beam focusing, the sextupole for chromaticity compensation, the octupole for field errors or field compensation [29]. Similarly, the toroidal multipole moments can be interpreted as dipole, quadrupole, sextupole, etc., field components [25]. Following the present work, these components will be deeply investigated in order to be able to predict them once the input parameters listed below are defined:

- number of the coils;
- shape and size of the coils;
- current.

6. Conclusion

This study investigates the multipolar expansion of the magnetic flux density in toroidal harmonics, with the main purpose of identifying a valid procedure for the calculation of the multipole coefficients.

Initially, it has been necessary to establish and examine the most appropriate coordinate system for this analysis. Despite its complexity, it can be stated that the recommended set of coordinates is the three-dimensional toroidal coordinate system identified by (ξ, η, ϕ), obtained by the rotation about the $z - axis$ of the two-dimensional coordinate system (ξ, η). The toroidal set of coordinates allows one to solve the Laplace's equation with a solution strategy known as *R-separation*. This is an essential requirement for the development of the multipole expansion, which is in fact obtained by solving the Laplace'equation for the scalar potential. However, in order to have a complete description of the magnetic flux density generated by a toroidal magnet, it has been necessary to add a particular function to this solution. This supplementary term is fundamental to describe the contribution of the magnetic field related to the currents flowing along the $z - axis$, which is not involved in the solution of the Laplace's equation.

From the expression of the scalar potential, the components of the magnetic field in toroidal coordinates were obtained; since these expressions involve the associated Legendre functions with half-integer indexes, it was necessary to verify their consistency by plotting them on MATLAB.

After all these studies, it was possible to develop a procedure for the evaluation of the multipole moments. The main requirement for the application of this method is the knowledge of the scalar potential on a set of points characterized by a constant value of ξ, for a specific toroidal magnet. These data were then fitted with three different equations in order to find the multipolar coefficients, with satisfactory precision. Regarding the research of the scalar potential on the reference points, it can be stated that the employment of the computational tool *Field 2017*, followed by a numerical integration, allows

one to reach this result this request with an acceptable computational effort.

No simplifications have been introduced in this description. This is due to the aim of providing a general analysis of the multipole expansion, suitable for the majority of the toroidal magnets.

In order to exploit the full potential of this work, in practical applications of toroids, future studies are needed to find the relation between the current distribution in the coils and the multipole moments.

7. Appendix A

A differential equation expressed in the form:

$$\frac{d}{dx}\left((1-x^2)\frac{d}{dx}P_n(x)\right)+n(n+1)P_n(x)=0$$

is called *Legendre's differential equation* and the correspondent solutions are called *Legendre functions* (or *Legendre polynomials*); they can be expressed by means of the Rodriguez formula:

$$P_n(x)=\frac{1}{2^n n!}\frac{d^n}{dx^n}(x^2-1)^n$$

If indeed the expression of the differential equation is written as:

$$(1-x^2)\frac{d^2}{dx^2}P_l^m(x)+\left[l(l+1)-\frac{m^2}{1-x^2}\right]P_l^m(x)=0$$

the equation is defined *Associated Legendre's differential equation* and consequently the solutions are called *Associated Legendre functions* [18]. Also in this case the solution is deduced from the Rodriguez formula and results:

$$P_l^m(x)=\frac{(-1)^m}{2^l l!}(1-x^2)^{m/2}\frac{d^{l+m}}{dx^{l+m}}(x^2-1)^l$$

Both of the mentioned functions have been widely studied and numerical values have been tabulated [30]. However, in some physical and mathematical problems, is requested the introduction of a new kind of Legendre function which involves fractional indexes. In these cases the differential equation to solve is expressed as follow:

$$\frac{d^2f}{d\xi^2}+\coth(\xi)\frac{df}{d\xi}+\left(\frac{1}{4}-m^2-\frac{n^2}{\sinh^2(\xi)}\right)f=0$$

and the correspondent general solution is:

$$f = \sum_{m=0}^{\infty} \sum_{n=0}^{\infty} \Big[A_{m,n} P^n_{m-\frac{1}{2}}(\cosh \xi) + B_{m,n} Q^n_{m-\frac{1}{2}}(\cosh \xi) \Big]$$

where $P^n_{m-\frac{1}{2}}(\cosh \xi)$ and $Q^n_{m-\frac{1}{2}}(\cosh \xi)$ are called *Legendre function with half-integer indexes* or also *Legendre polynomials of fractional degree*, of the first and of the second kind, respectively. $A_{m,n}$ and $B_{m,n}$ are coefficients to be determined.

Regarding the Legendre function of the first kind $P^n_{m-\frac{1}{2}}(\cosh \xi)$, it diverges when $\cosh(\xi) = \infty$, that corresponds to $\xi = \infty$. While the Legendre function of the second kind presents a singularity if $\cosh(\xi) = 1$, which corresponds to $\xi = 0$.

At the moment, there are no standard computer library routines available for the evaluation of this kind of Legendre polynomials. One of the most exploited strategy for their computation involves the hypergeometric function $F(a, b; c; z)$ and is briefly described below [18].

The half-integer Legendre functions can be expressed in terms of the hypergeometric function $F(a, b; c; z)$.

$$P^n_{m-\frac{1}{2}}(\cosh \xi) = \frac{\Gamma(m + n + \frac{1}{2})}{2^n n! \Gamma(m - n + \frac{1}{2})} \tanh^n \xi \cosh^{m-\frac{1}{2}} \xi \times F\left(\frac{1}{2}\Big(n - m + \frac{1}{2}\Big), \frac{1}{2}\Big(n - m + \frac{3}{2}\Big); n + 1; \tanh^2 \xi \right)$$

$$Q^n_{m-\frac{1}{2}}(\cosh \xi) = \frac{\Gamma(\frac{1}{2})\Gamma(m + n + \frac{1}{2})}{2^{m+\frac{1}{2}} \Gamma(m + 1)} \frac{\tanh^n \xi}{\cosh^{m+\frac{1}{2}\frac{1}{2}} \xi} \times F\left(\frac{1}{2}\Big(m + n + \frac{1}{2}\Big), \frac{1}{2}\Big(m + n + \frac{3}{2}\Big); m + 1; \frac{1}{\cosh^2 \xi} \right)$$

The hypergeometric function $F(a, b; c; z)$ can be expanded as a series. The terms a, b, c, z are all real and $0 < z < 1$.

$$F(a, b; c; z) = \sum_{i=0}^{\infty} S(i)$$

where

$$S(i) = \frac{(a + i - 1)(b + i - 1)}{(c + i - 1)} \frac{z}{i} S(i - 1)$$

with $i \geq 1$ and $S(0) = 1$.

The following definitions can be used for the evaluation of the derivatives of $P^n_{m-\frac{1}{2}}(\cosh \xi)$ and $Q^n_{m-\frac{1}{2}}(\cosh \xi)$, respectively.

$$\frac{\partial}{\partial \xi} Q^n_{m-\frac{1}{2}}(\cosh \xi) = \frac{(m - \frac{1}{2})}{\tanh(\xi)} Q^n_{m-\frac{1}{2}}(\cosh \xi) - \frac{(n + m - \frac{1}{2})}{\sinh(\xi)} Q^n_{m-\frac{3}{2}}(\cosh \xi)$$

$$\frac{\partial}{\partial \xi} P^n_{m-\frac{1}{2}}(\cosh \xi) = \frac{(m - \frac{1}{2})}{\tanh(\xi)} P^n_{m-\frac{1}{2}}(\cosh \xi) - \frac{(n + m - \frac{1}{2})}{\sinh(\xi)} P^n_{m-\frac{3}{2}}(\cosh \xi)$$

Bibliography

[1] Paul H Schimpf. "A Detailed Explanation of Solenoid Force". In: *International Journal on Recent Trends in Engineering & Technology* 8.2 (2013), p. 7.

[2] Vijay Gangadhar Phadke. *Insulation and integrated heat sink for high frequency, low output voltage toroidal inductors and transformers*. US Patent 7,142,085. 2006.

[3] Pascal Tixador. "Superconducting magnetic energy storage: Status and perspective". In: *IEEE/CSC&ESAS European Superconductivity News Forum*. 3. 2008.

[4] Neil Mitchell, Arnaud Devred, et al. "The ITER magnet system: Configuration and construction status". In: *Fusion Engineering and Design* 123 (2017), pp. 17–25.

[5] A. Foussat, H. H. J. Ten Kate, B. Levesy, C. Mayri, Y. Pabot, V. Petrov, M. Raymond, Z. Sun, and P. Vedrine. "Assembly Concept and Technology of the ATLAS Barrel Toroid". In: *IEEE Transactions on Applied Superconductivity* 16.2 (2006), pp. 565–569.

[6] JA Macdonald, M Abe, M Aoki, I Arai, Y Asano, T Baker, M Blecher, MD Chapman, P Depommier, P Gumplinger, et al. "Apparatus for a search for T-violating muon polarization in stopped-kaon decays". In: *Nuclear Instruments and Methods in Physics Research Section A: Accelerators, Spectrometers, Detectors and Associated Equipment* 506.1-2 (2003), pp. 60–91.

[7] Bernhard A Mecking, G Adams, S Ahmad, E Anciant, M Anghinolfi, B Asavapibhop, G Asryan, G Audit, T Auger, H Avakian, et al. "The CEBAF large acceptance spectrometer (CLAS)". In: *Nuclear Instruments*

and Methods in Physics Research Section A: Accelerators, Spectrometers, Detectors and Associated Equipment 503.3 (2003), pp. 513–553.

[8] Simon van der Meer. *A directive device for charged particles and its use in an enhanced neutrino beam*. Tech. rep. Cern, 1961.

[9] V. Calvelli, R. Musenich, F. Tunesi, and R. Battiston. "A Novel Configuration for Superconducting Space Radiation Shields". In: *IEEE Transactions on Applied Superconductivity* 27.4 (2017).

[10] W.D. D'haeseleer, W.N.G. Hitchon, J.D. Callen, and J.L. Shohet. *Flux Coordinates and Magnetic Field Structure*. Springer Series in Compuational Physics, 1991.

[11] P. Moon and D. E. Spencer. *Field Theroy Handbook*. Springer, Berlin, Heidelberg, 1961.

[12] G.B. Arfken, H. J. Weber, and F. E. Harris. *Mathematical Methods for Physicists*. 7th edition. Academic Press, 2012.

[13] A. R Edmonds. *Angular momentum in quantum mechanics*. English. 3d print., with corrections. Includes index. Princeton, N.J. : Princeton University Press, 1974.

[14] Stephan Russenschuck. *Field computation for accelerator magnets: analytical and numerical methods for electromagnetic design and optimization*. John Wiley & Sons, 2011.

[15] J Herrera, G Ganetis, R Hogue, E Rogers, P Wanderer, and E Willen. "Measurement of the magnetic field coefficients of particle accelerator magnets". In: *Particle Accelerator Conference, 1989. Accelerator Science and Technology., Proceedings of the 1989 IEEE*. IEEE. 1989, pp. 1774–1776.

[16] S. Turner. *Measurement and Alignment of Accelerator and Detector Magnets: Cern Accelerator School: Europa Palace Hotel, Anacapri, Italy, 11-17 April 1997: Proceedings*. CERN (Series). CERN, European Organization for Nuclear Research, 1998.

[17] Steven W Smith et al. "The scientist and engineer's guide to digital signal processing". In: (1997).

[18] Milton Abramowitz and Irene A Stegun. *Handbook of mathematical functions: with formulas, graphs, and mathematical tables*. Vol. 55. Courier Corporation, 1964.

[19] Philip McCord Morse and Herman Feshbach. *Methods of theoretical physics*. Technology Press, 1946.

[20] F Alladio and F Crisanti. "Analysis of MHD equilibria by toroidal multipolar expansions". In: *Nuclear Fusion* 26.9 (1986), p. 1143.

[21] GH Neilson and JH Harris. "Harmonic analysis for magnetic configuration control in experimental stellarator devices". In: *Nuclear fusion* 27.5 (1987), p. 711.

[22] W Dommaschk. "Representations for vacuum potentials in stellarators". In: *Computer physics communications* 40.2-3 (1986), pp. 203–218.

[23] L Brouwer, S Caspi, D Robin, and W Wan. "3D toroidal field multipoles for curved accelerator magnets". In: (2017).

[24] J Segura and A Gil. "Evaluation of toroidal harmonics". In: *Computer Physics Communications* 124.1 (2000), pp. 104–122.

[25] B Ph Van Milligen and A Lopez Fraguas. "Expansion of vacuum magnetic fields in toroidal harmonics". In: *Computer physics communications* 81.1-2 (1994), pp. 74–90.

[26] Lucas Nathan Brouwer. *Canted-cosine-theta superconducting accelerator magnets for high energy physics and ion beam cancer therapy*. University of California, Berkeley, 2015.

[27] Jeoren van Nugteren. *Internship Report: CERN, Software development for the Science and Design behind Superconducting Magnet Systems*. Twente University: Energy Materials, Systems, and CERN: ATLAS magnet team. Tech. Rep., 2011.

[28] W Hafla, A Buchau, and WM Rucker. "Efficient computation of source magnetic scalar potential". In: *Advances in Radio Science: ARS* 4 (2006), p. 59.

[29] Klaus Wille. *The physics of particle accelerators: an introduction*. Clarendon Press, 2000.

[30] Solomon L'vovich Belousov. *Tables of Normalized Associated Legendre Polynomials: Mathematical Tables Series*. Elsevier, 2014.